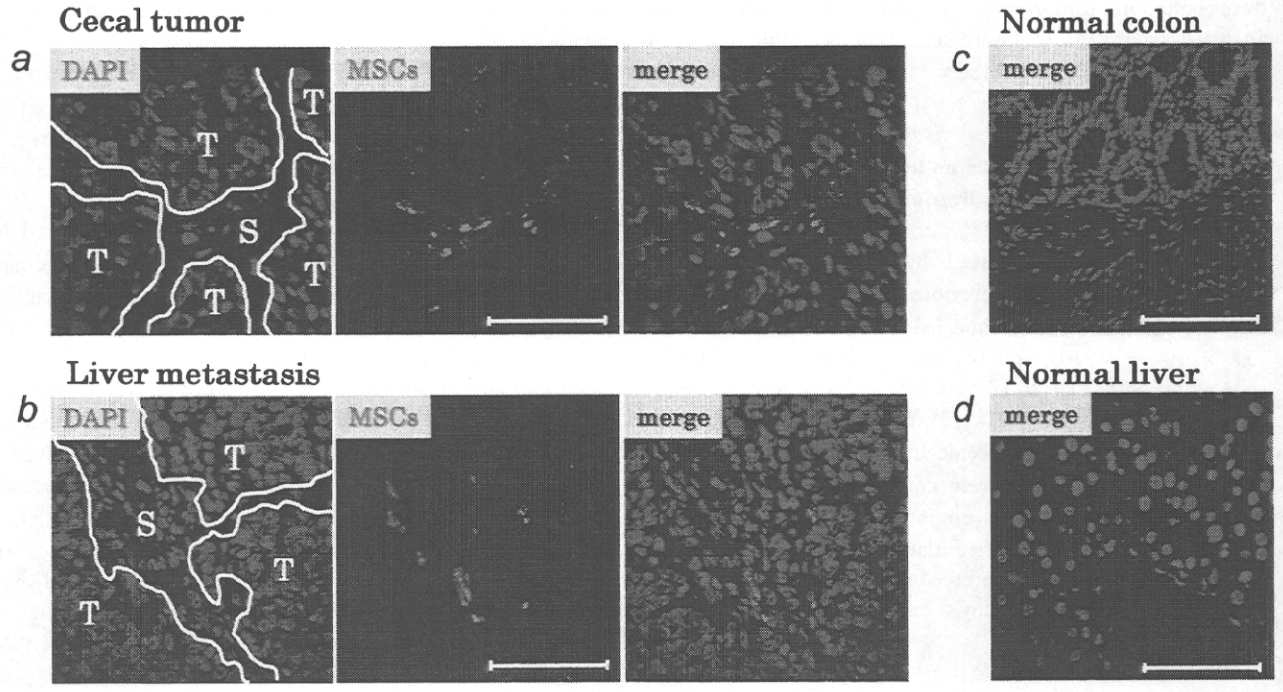

Figure 1. Migration of circulating MSCs to the stromata of orthotopic colon tumor and metastatic liver tumor. Systemically administered MSCs possess the ability to migrate to the orthotopic colon tumor stroma (*a*) and metastatic liver tumor (*b*). 4′,6-Diamidino-2-phenylindole (DAPI) staining for cell nuclei (blue) shows the outline of the stroma within tumor tissue. PKH26-labeled MSCs (red) are detected specifically in the tumor stroma but not in the noncancerous tissues, such as normal colon and normal liver (*c* and *d*). T: tumor nest; S: stroma; Scale bars: 100 μm.

seeded in a 12-well plate, and the next day, control medium or MSC-conditioned medium was added (day 0). The medium was changed on days 2 and 4, and the number of cells was counted on days 2, 4 and 7 ($n = 6$ in each group).

Migration assay

The migratory ability of KM12SM cells was assayed with the use of a 12-well microchamber plate with uncoated inserts (12-μm pore size, Corning Costar, Tokyo, Japan). Either 1.0×10^5 MSCs in DMEM with 0.5% FBS or the medium alone was plated into the lower chambers. After 24 hr of incubation at 37°C, upper chambers containing 1.0×10^5 KM12SM cells in DMEM with 0.5% FBS were set into the lower chambers. Three wells were used for each experiment. After 48 hr of incubation at 37°C, inserts were fixed with 10% buffered formalin solution and stained with hematoxylin. The cells on the upper surface of the membranes were removed with cotton swabs. The number of migrating cells was counted in three random fields per filter at 200× magnification.

The migratory ability of MSCs was also assayed by means of a 24-well microchamber plate with uncoated inserts (8-μm pore size, Corning Costar). Either 2.0×10^4 KM12SM in DMEM with 0.5% FBS or medium alone was plated into the lower chambers. After 4 hr of incubation at 37°C, upper chambers containing 2.0×10^4 MSCs in DMEM with 0.5% FBS were set into the lower chambers. Three wells were used for each experiment. After 16 hr of incubation at 37°C, inserts were fixed with 10% buffered formalin solution and stained with hematoxylin. The number of migrating cells was determined as described above.

Invasion assay

The invasive ability of KM12SM cells was assayed by using a 24-well microchamber plate (12 μm pore size, Corning Costar) according to a previously described method,[31] but with minor modifications. In brief, the upper surface of each membrane was coated with Matrigel (240 μg per filter, BD Biosciences, San Jose, CA). KM12SM (1.0×10^5) cells were seeded in the upper chamber with serum free medium, and MSC-conditioned medium or control medium was added to the lower chambers. Three wells were used for each experiment. After 46 hr of incubation at 37°C, inserts were treated as in the migration assay. The number of invading cells was counted in three random fields per filter at 100× magnification.

Statistical analysis

Survival curves were drawn by the Kaplan and Meier method, and the log rank test was used to analyze differences in survival rates. Student's or Welch's *t*-test or the Wilcoxon test was used to analyze differences in other variables, as appropriate. Data are expressed as mean ± standard error

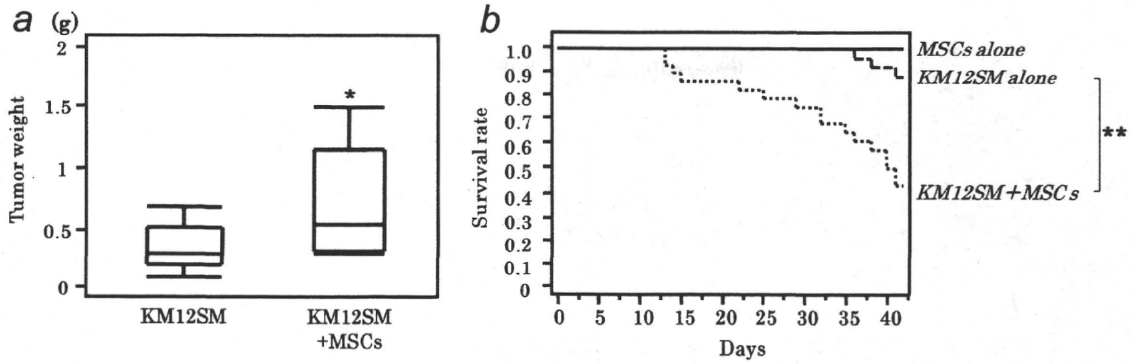

c

Liver metastasis \ Transplanted cells	KM12SM alone	KM12SM +MSCs
+	0	2
—	21	10
Total number of mice	21	12

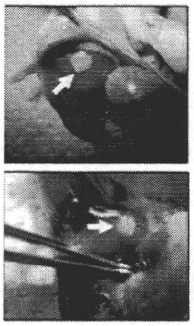

Figure 2. (*a*) Transplantation of KM12SM cells mixed with MSCs (0.5×10^6:1.0×10^6, $n = 12$ mice) resulted in significantly greater tumor weight than that resulting from transplantation of KM12SM cells alone (0.5×10^6, $n = 21$). *$p < 0.05$, Bars: SE. (*b*) Kaplan–Meier curves show survival of mice bearing KM12SM cells alone ($n = 24$), KM12SM cells mixed with MSCs ($n = 28$) and MSCs alone ($n = 10$). The survival rate was significantly lower in the mixed-cell group. *p* values were determined by log-rank test. **$p < 0.001$. (*c*) Macroscopic liver metastasis was seen only in the group that received KM12SM cells mixed with MSCs. Arrows denote macroscopic liver metastases.

(SE). Probability values of <0.05 were considered significant. All statistical analyses were performed with JMP software (SAS Institute, Cary, NC).

Results

Migration of MSCs to the stroma of orthotopic primary tumors and to metastatic liver tumors

After injection of PKH-labeled MSCs into the tail veins of tumor-bearing mice, MSCs were detected specifically in the tumor stroma (Fig. 1*a*) at the primary site. MSCs were also detected in the stroma of metastatic liver tumors (Fig. 1*b*). In contrast, MSCs were not detected in the noncancerous tissues, such as normal colonic mucosa and liver (Figs. 1*c* and 1*d*).

Promotion of the growth of orthotopic colon tumors by MSCs

At 6 weeks after transplantation of KM12SM cells alone, KM12SM cells mixed with MSCs, or MSCs alone into the cecal wall of nude mice, the weight of tumors resulting from mixed cells was significantly greater than the weight of tumors resulting from tumor cells alone (0.47 ± 0.10 *vs.* 1.03 ± 0.38 g, $p < 0.05$; Fig. 2*a*). The survival rate was significantly lower in the mixed-cell group than in the group that received KM12SM cells alone ($p < 0.001$; Fig. 2*b*). MSCs alone did not have the ability to generate any tumor and did not affect the survival of mice. Surviving mice were killed on day 42. Liver metastasis was not seen macroscopically in the 21 mice that received tumor cells alone, but liver metastasis was seen macroscopically in two of the 12 mice in the mixed-cell group (Fig. 2*c*). To clarify the mechanisms underlying the growth-promoting effect, we examined proliferation, apoptosis and angiogenesis in primary tumors by immunohistochemistry. The PCNA-LI, AI and MVA were compared between the tumors resulting from transplantation of KM12SM cells alone and those resulting from transplantation of KM12SM cells mixed with MSCs. The PCNA-LI was significantly higher (42.0 ± 5.3 *vs.* 62.9 ± 4.6 %, $p < 0.05$; Fig. 3*a*) and the AI was significantly lower in the mixed-cell group (7.0 ± 0.6 *vs.* 3.4 ± 0.3 %, $p < 0.001$; Fig. 3*b*). The MVA was significantly greater in the tumors from the mixed-cell group (13,719 ± 2,154 *vs.* 24,594 ± 2,230 μm^2, $p < 0.01$; Fig. 3*c*).

Differentiation of MSCs in orthotopic colon tumors

Three weeks after transplantation of KM12SM cells mixed with PKH26-labeled MSCs, commingled MSCs were incorporated into the tumor stroma and expressed α-SMA, PDGFR-β, desmin, FSP and FAP as CAF markers (Fig. 4*a*), but they did not express human CD31 (data not shown). The

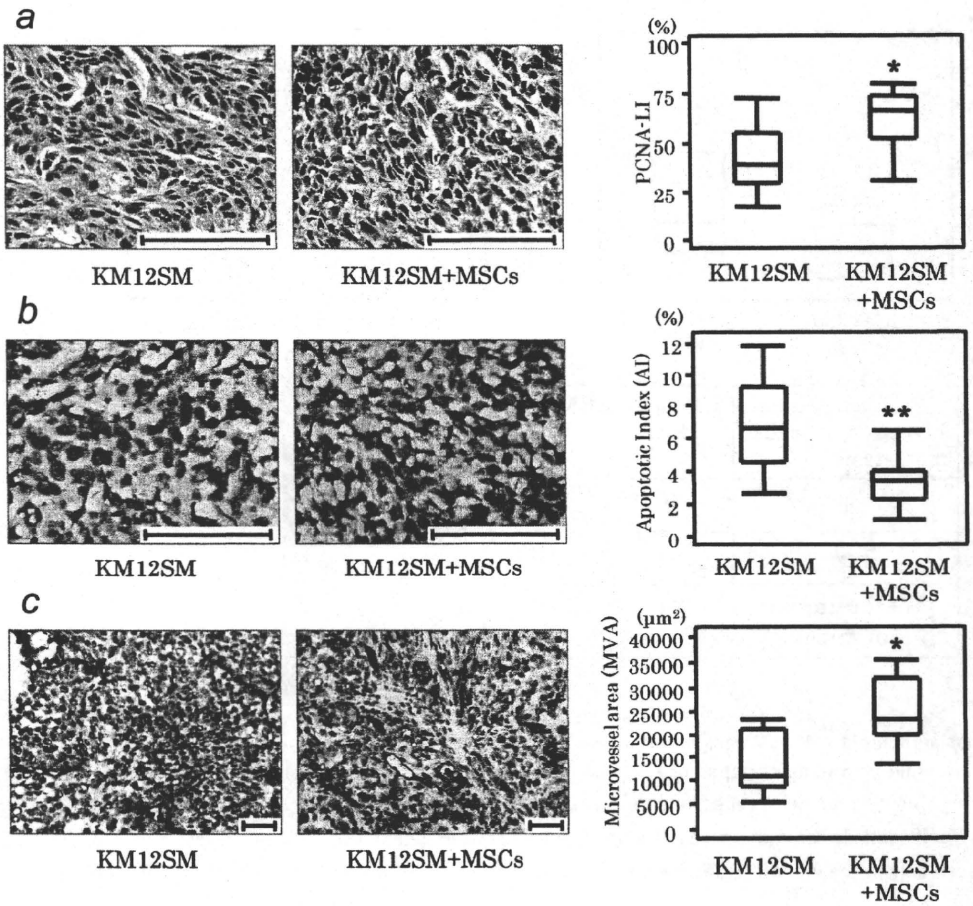

Figure 3. MSCs enhance proliferation and angiogenesis and inhibit apoptosis *in vivo*. (*a*) Proliferative activity was evaluated by the proliferating cell nuclear antigen labeling index (PCNA-LI, %). The PCNA-LI was significantly higher in tumors from the mixed-cell group than in tumors from the group that received KM12SM cells alone. (*b*) Apoptotic cells in tumors were detected by the terminal deoxynucleotide transferase-mediated dUTP-biotin nick end labeling method, and the apoptotic index (AI, %) was calculated. The AI was significantly lower in tumors from the mixed-cell group than in tumors from the group that received KM12SM cells alone. (*c*) Tumor microvessel areas (MVAs) were calculated. The MVA was significantly greater in tumors from the mixed-cell group. *$p < 0.01$, Bars: SE. **$p < 0.001$, Bars: SE. Scale bars: 100 μm

morphology and distribution of MSCs within tumor stroma were similar to those of CAFs. Before the introduction of MSCs into mice, we examined the expression of α-SMA and PDGFR-β in MSCs during *in vitro* propagation. MSCs expressed PDGFR-β at a low level but not α-SMA (Fig. 4*b*).

Increase in the number of liver metastases by injection of KM12SM cells mixed with MSCs

Transplantation of KM12SM cells mixed with MSCs into the spleen of nude mice resulted in a significantly greater number of liver metastases at 4 weeks than that resulting from transplantation of KM12SM cells alone (2.6 ± 4.3 *vs.* 15.1 ± 6.0, $p < 0.01$; Fig. 5*a*). In addition, commingled MSCs migrated to the stroma of metastatic liver tumors and expressed α-SMA, PDGFR-β, desmin, FAP and FSP as CAF markers (Fig. 5*b*).

Attraction between KM12SM cells and MSCs *in vitro*

To investigate whether KM12SM cells have the ability to attract MSCs *in vitro*, migration assay was performed. We found that more human MSCs migrated toward the KM12SM cell culture than toward the medium without KM12SM cells (30.9 ± 3.5 *vs.* 24.2 ± 3.6 cells/field, $p < 0.05$; Fig. 6*a*).

We then examined the effects of MSCs on migration and invasion of KM12SM cells. The ability of KM12SM cells to migrate toward the MSC culture was significantly greater than the ability of these cells to migrate toward the medium without MSCs (114.9 ± 16.1 *vs.* 170.2 ± 18.5 cells/field, $p < 0.05$; Fig. 6*b*). Moreover, the invasive ability of KM12SM cells was significantly greater toward MSC-conditioned medium than toward control medium (33.1 ± 7.4 *vs.* 59.0 ± 7.9 cells/field, $p < 0.05$; Fig. 6*c*).

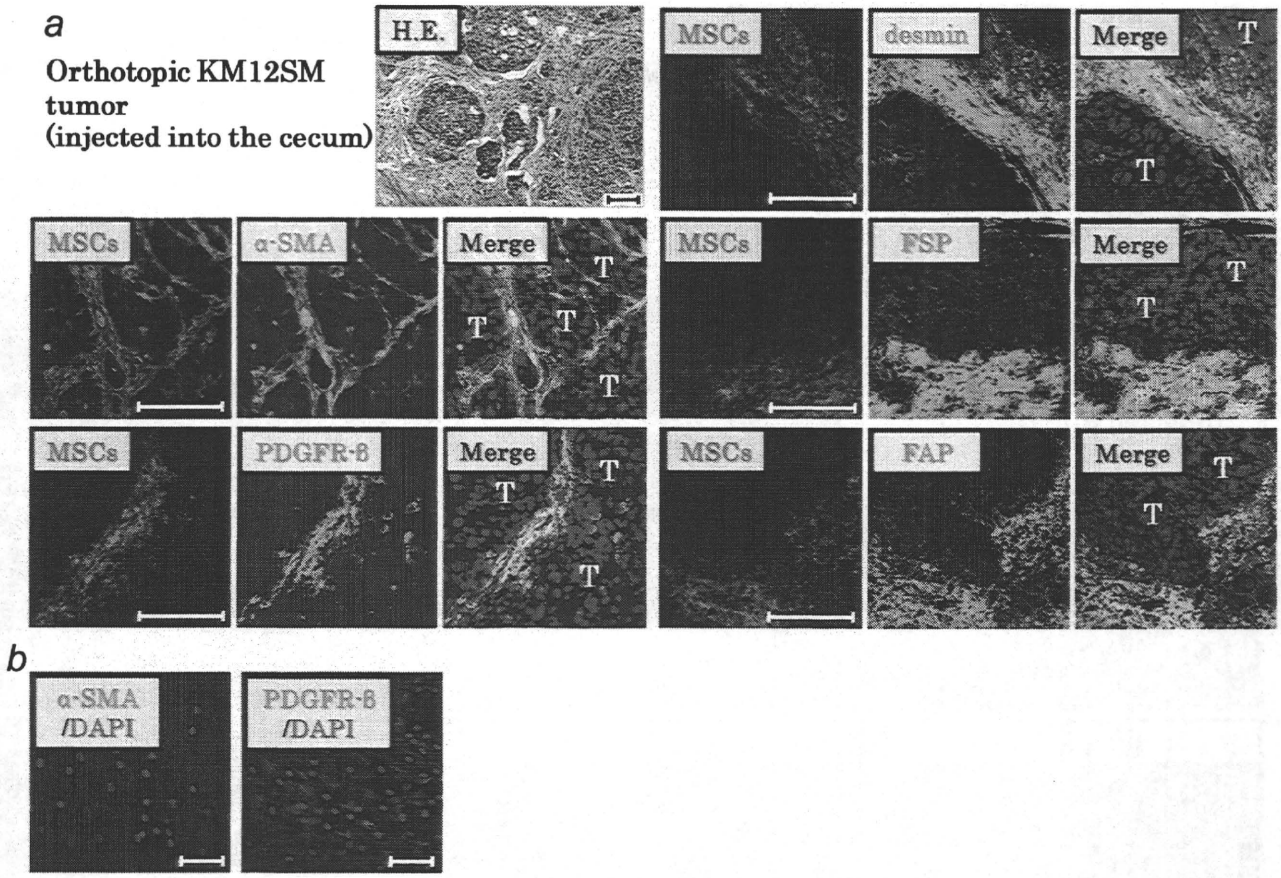

Figure 4. (*a*) Immunofluorescence staining for α-SMA, PDGFR-β, desmin, FSP or FAP (green) was performed in the orthotopic colon tumors resulting from KM12SM cells mixed with PKH26-labeled MSCs (red). Commingled MSCs were incorporated into the tumor stroma and expressed α-SMA, PDGFR-β, desmin, FSP and FAP. (*b*) Immunofluorescence staining for α-SMA and PDGFR-β was performed in MSCs cultured on slide glass. There was no α-SMA expression and low PDGFR-B expression in the cultured MSCs. T: tumor nest; Scale bars: 100 μm

The effect of the soluble factors secreted from MSCs on the proliferation of KM12SM cells was also examined. KM12SM cells were exposed to control medium or MSC-conditioned medium and then counted on days 2, 4 and 7. No significant difference was observed in the number of KM12SM cells between the two groups at any time point (Fig. 6*d*).

Discussion

It has been reported that MSCs migrate to a variety of tumors, such as melanomas,[32,33] gliomas[34,35] and colon,[14,36] pancreatic[37,38] and breast cancers.[10,33,39,40] Studies have implicated molecules such as CXCL12 (SDF-1)/CXCR4,[36] CCL2 (MCP-1)/CCR2[39] and PDGF[37] in the tumor-homing ability of MSCs. In the present study, we showed that circulating MSCs have the ability to migrate not only to the stroma of orthotopic colon tumors but also to metastatic lesions. In *in vitro* experiments, we observed that tumor cells recruit MSCs through the release of soluble factors. Although the exact molecular mechanisms that govern MSC migration are not fully characterized, this migratory ability points to MSCs as attractive candidates for delivery vehicles of antitumor agents.[32–35] However, several coinjection experiments have revealed that MSCs promote tumor growth and metastasis,[5–13] which would present a serious obstacle to using MSCs as delivery vehicles for anti-cancer therapy. Thus, the precise effects of MSCs on tumor growth and progression and the mechanism underlying these effects should be elucidated.

We previously reported that expression of metastasis-related genes by cancer cells and stromal cells is higher in orthotopic (cecal wall) KM12SM human colon carcinomas than in ectopic (subcutaneous) tumors.[15,16,25] The stromal reaction and metastatic potential are increased in the orthotopic microenvironment. Therefore, orthotopic models should be used to study tumor–stroma or tumor–MSC interaction.[21,23,41,42] In our study, orthotopic transplantation of tumor cells mixed with MSCs into the cecal wall, in comparison to orthotopic transplantation of tumor cells alone, resulted in significantly greater tumor weight. In primary tumors, PCNA-LI (proliferation) and MVA (angiogenesis)

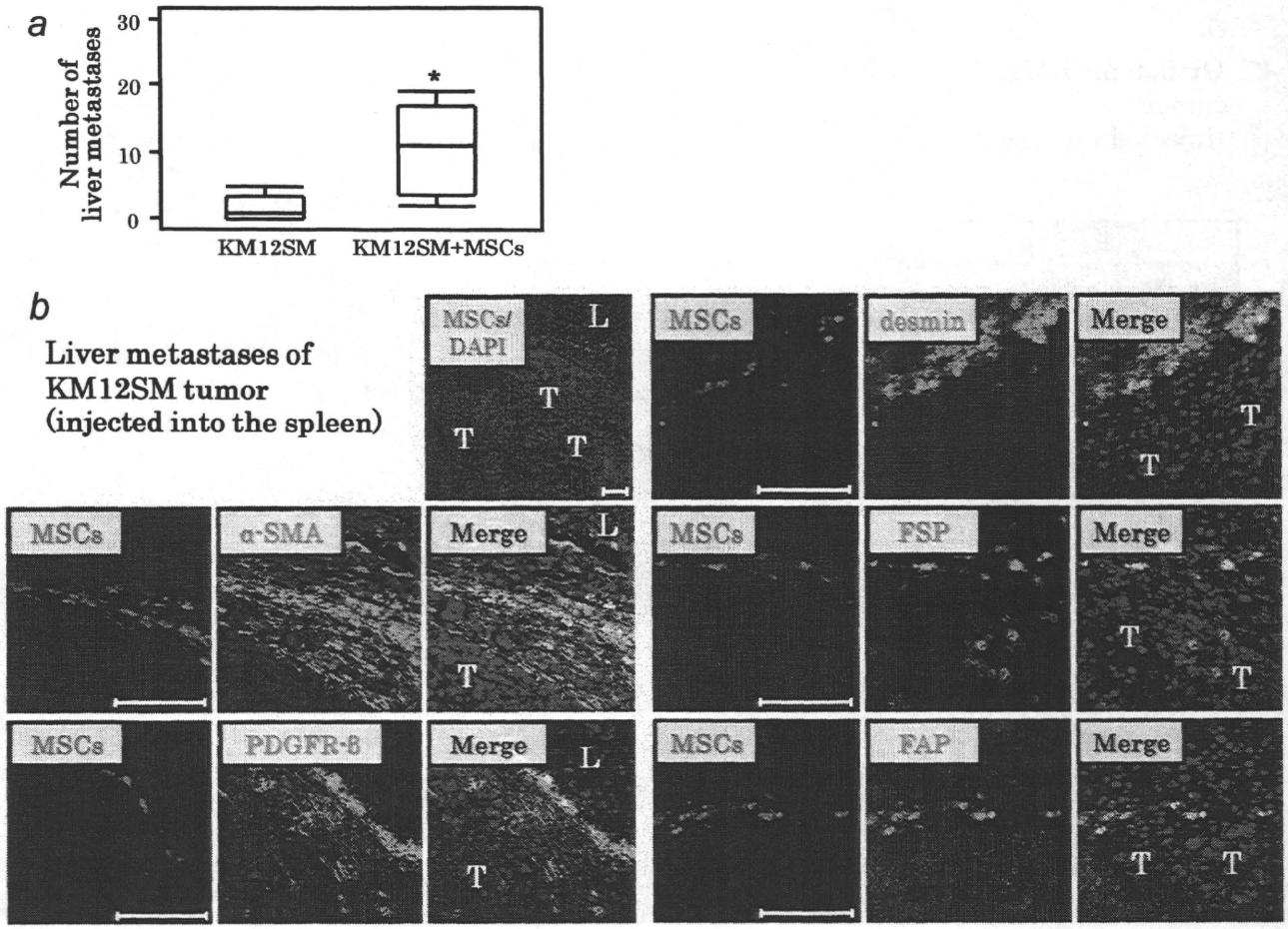

Figure 5. (*a*) Transplantation of KM12SM cells mixed with MSCs (0.5×10^6:1.0×10^6, $n = 10$) resulted in a significantly greater number of liver metastases than the number resulting from transplantation of KM12SM cells alone (0.5×10^6, $n = 10$). *$p < 0.01$, Bars: SE. (*b*) Immunofluorescence staining for α-SMA, PDGFR-β, desmin, FSP and FAP (green) was performed in metastatic liver tumors resulting from KM12SM cells mixed with PKH26-labeled MSCs (red) injected into the spleen. Commingled MSCs migrated to the stroma of metastatic liver tumors and expressed α-SMA, PDGFR-β, desmin, FSP and FAP. L: normal liver, T: tumor nest; Scale bars: 100 μm.

were significantly increased, and the AI (apoptosis) was significantly lower in the tumors from the mixed-cell group. More intriguingly, macroscopic liver metastasis appeared only in the mixed-cell group, and the survival rate was significantly lower in this group. MSCs promoted migration and invasion of KM12SM cells *in vitro*. Because MSCs enhance proliferation, angiogenesis, migration and invasion and inhibit apoptosis of tumor cells, they may promote tumor growth and metastasis, which are followed by decreased survival. These findings are consistent with previously reported findings.[6,7,11]

In addition, we found commingled MSCs were functionally incorporated into the stroma of orthotopic colon tumors, where they expressed α-SMA, PDGFR-β, desmin, FAP and FSP as CAF markers. These results appear to corroborate the *in vitro* findings of Mishra *et al.*, who showed that MSCs exposed to tumor-conditioned medium for 30 days can act as CAF-like cells.[12,13] CAFs are known to promote tumor growth and metastasis, and phenotypes of CAFs are distinct from those of normal fibroblasts.[43,44] CAFs may arise from fibroblasts residing in local tissues,[18] periadventitial cells including pericytes and vascular smooth muscle cells,[45] endothelial cells[46] or bone marrow–derived cells including various stem cells.[47] MSCs differentiate by nature into tissues of mesodermal origin, so it is reasonable to suppose that CAFs derive from MSCs.

To more specifically determine the effect of MSCs on metastasis *in vivo*, we used an experimental liver metastasis model, and we found that MSCs enhanced the metastatic potential of KM12SM cells. The number of liver metastases was increased by coimplantation with MSCs; thus, MSCs may affect colonization step and maintain cancer cells. MSCs commingled with tumor cells at the primary tumor site (spleen) were able to travel to the stroma of metastatic foci in the liver, where they expressed CAF markers. These findings indicate that MSCs support tumor metastasis not only at the primary site but also at metastatic sites.

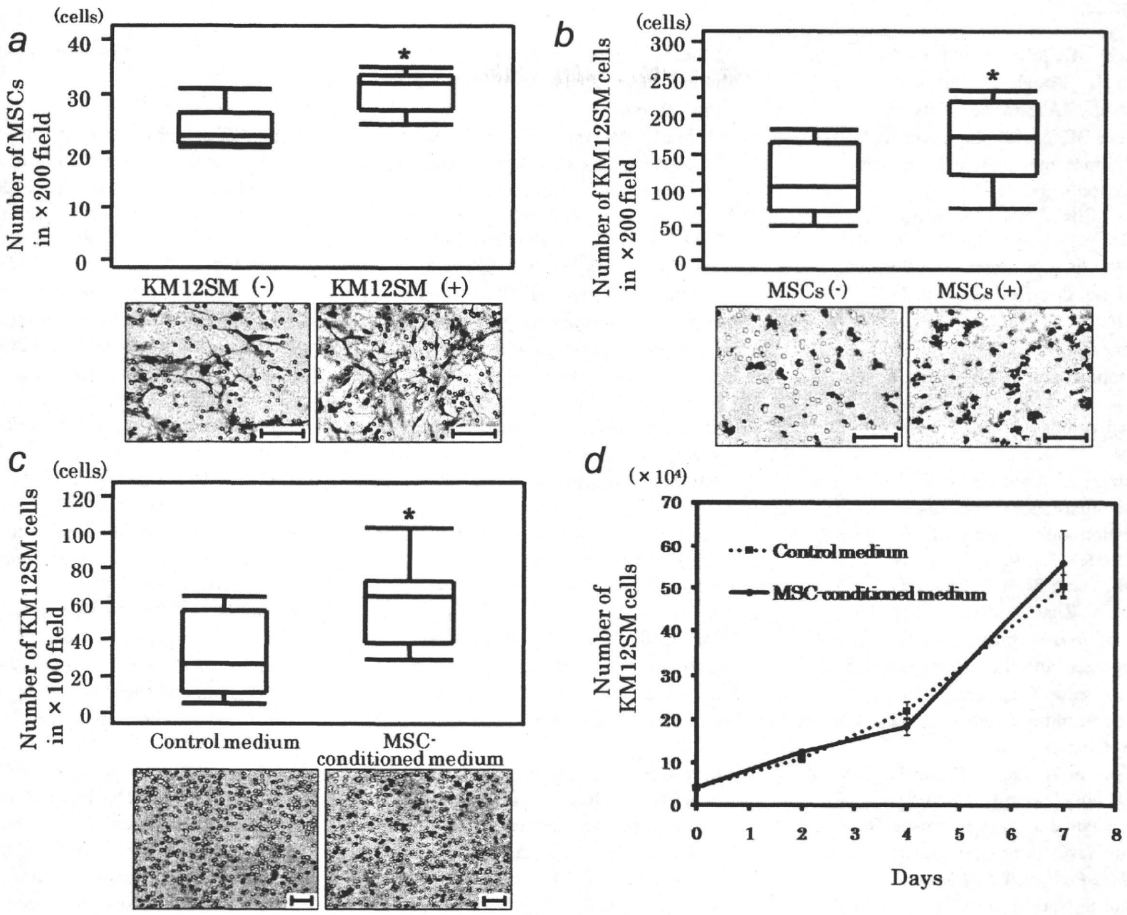

Figure 6. Interactions between KM12SM cells and MSCs *in vitro*. (*a*) The migratory ability of MSCs was analyzed by transwell assay. A significantly greater number of MSCs migrated toward the culture of KM12SM cells than toward the medium without KM12SM cells. (*b*) The migratory ability of KM12SM cells was also stimulated by coculture with MSCs. KM12SM cells were plated into upper chambers, which were then set into the lower chambers with or without MSCs. More KM12SM cells migrated toward the culture of MSCs than toward the medium without MSCs. (*c*) Effect of MSCs on the invasion of KM12SM cells. KM12SM cells were seeded in the upper chambers with serum free medium, and MSC-conditioned medium or control medium was added to the lower chambers. More KM12SM cells invaded Matrigel toward MSC-conditioned medium than toward control medium. Lower panels are typical photographs of the assay. $*p < 0.05$, Bars: SE. Scale bars: 100 μm. (*d*) Proliferation curves. KM12SM cells were exposed to control medium or MSC-conditioned medium and then counted on days 2, 4 and 7. No significant difference was observed in the number of cells between groups at any time point.

Karnoub *et al.* reported that CCL5 secreted from MSCs acts on the CCR5 of breast cancer cells only at the primary site and temporarily promotes lung metastasis without influencing primary tumor growth and neoangiogenesis[10]; in fact, MSCs did not exist at the sites of lung metastasis. They speculated that the enhanced metastatic ability was due to enhanced extravasation and colonization of cancer cells at the metastatic site. They also showed that MSCs promoted lung metastasis of all breast cancer cell lines used in their study, but the growth kinetics of MSC-containing tumors at the primary sites differ between each breast cancer cell line. Thus, differences in experimental conditions, such as the kinds of cell lines and the sites (ectopic or orthotopic) of transplantation, may influence growth and angiogenesis of the primary tumors.

Our data indicate that MSCs may directly encourage tumor cells at the primary site to metastasize to the liver and that metastasized tumor cells may in turn recruit MSCs to metastatic sites where the MSCs differentiate into supporting CAF-like cells. Understanding the molecular mechanisms of interaction between tumor cells and MSCs could lead to establishment of new therapies for targeting tumor stroma at both primary and metastatic sites. Orthotopic transplantation models should be used in *in vivo* studies of tumor–MSC interactions for the design of anticancer therapies.

Acknowledgements

The authors thank Ms. Megumi Wakisaka, Mr. Shinichi Norimura, and Ms. Emiko Hisamoto for their excellent technical assistance. This work was carried out with the kind cooperation of the Analysis Center of Life Science, Hiroshima University (Hiroshima, Japan).

References

1. Pittenger MF, Mackay AM, Beck SC, Jaiswal RK, Douglas R, Mosca JD, Moorman MA, Simonetti DW, Craig S, Marshak DR. Multilineage potential of adult human mesenchymal stem cells. *Science* 1999;284:143–7.
2. Fox JM, Chamberlain G, Ashton BA, Middleton J. Recent advances into the understanding of mesenchymal stem cell trafficking. *Br J Haematol* 2007;137: 491–502.
3. Gregory CA, Prockop DJ, Spees JL. Non-hematopoietic bone marrow stem cells: molecular control of expansion and differentiation. *Exp Cell Res* 2005;306: 330–5.
4. Dvorak HF. Tumors: wounds that do not heal. Similarities between tumor stroma generation and wound healing. *N Engl J Med* 1986;315:1650–9.
5. Sun B, Zhang S, Ni C, Zhang D, Liu Y, Zhang W, Zhao X, Zhao C, Shi M. Correlation between melanoma angiogenesis and the mesenchymal stem cells and endothelial progenitor cells derived from bone marrow. *Stem Cells Dev* 2005;14:292–8.
6. Zhu W, Xu W, Jiang R, Qian H, Chen M, Hu J, Cao W, Han C, Chen Y. Mesenchymal stem cells derived from bone marrow favor tumor cell growth in vivo. *Exp Mol Pathol* 2006;80:267–74.
7. Annabi B, Naud E, Lee YT, Eliopoulos N, Galipeau J. Vascular progenitors derived from murine bone marrow stromal cells are regulated by fibroblast growth factor and are avidly recruited by vascularizing tumors. *J Cell Biochem* 2004;91:1146–58.
8. Djouad F, Bony C, Apparailly F, Louis-Plence P, Jorgensen C, Noel D. Earlier onset of syngeneic tumors in the presence of mesenchymal stem cells. *Transplantation* 2006;82:1060–6.
9. Djouad F, Plence P, Bony C, Tropel P, Apparailly F, Sany J, Noel D, Jorgensen C. Immunosuppressive effect of mesenchymal stem cells favors tumor growth in allogeneic animals. *Blood* 2003;102: 3837–44.
10. Karnoub AE, Dash AB, Vo AP, Sullivan A, Brooks MW, Bell GW, Richardson AL, Polyak K, Tubo R, Weinberg RA. Mesenchymal stem cells within tumour stroma promote breast cancer metastasis. *Nature* 2007;449:557–63.
11. Ramasamy R, Lam EW, Soeiro I, Tisato V, Bonnet D, Dazzi F. Mesenchymal stem cells inhibit proliferation and apoptosis of tumor cells: impact on in vivo tumor growth. *Leukemia* 2007;21:304–10.
12. Mishra PJ, Mishra PJ, Humeniuk R, Medina DJ, Alexe G, Mesirov JP, Ganesan S, Glod JW, Banerjee D. Carcinoma-associated fibroblast-like differentiation of human mesenchymal stem cells. *Cancer Res* 2008;68:4331–9.
13. Mishra PJ, Mishra PJ, Glod JW, Banerjee D. Mesenchymal stem cells: flip side of the coin. *Cancer Res* 2009;69:1255–8.
14. Hung SC, Deng WP, Yang WK, Liu RS, Lee CC, Su TC, Lin RJ, Yang DM, Chang CW, Chen WH, Wei HJ, Gelovani JG. Mesenchymal stem cell targeting of microscopic tumors and tumor stroma development monitored by noninvasive in vivo positron emission tomography imaging. *Clin Cancer Res* 2005;11:7749–56.
15. Kitadai Y, Sasaki T, Kuwai T, Nakamura T, Bucana CD, Fidler IJ. Targeting the expression of platelet-derived growth factor receptor by reactive stroma inhibits growth and metastasis of human colon carcinoma. *Am J Pathol* 2006;169:2054–65.
16. Kitadai Y, Sasaki T, Kuwai T, Nakamura T, Bucana CD, Hamilton SR, Fidler IJ. Expression of activated platelet-derived growth factor receptor in stromal cells of human colon carcinomas is associated with metastatic potential. *Int J Cancer* 2006;119: 2567–74.
17. Orimo A, Gupta PB, Sgroi DC, Arenzana-Seisdedos F, Delaunay T, Naeem R, Carey VJ, Richardson AL, Weinberg RA. Stromal fibroblasts present in invasive human breast carcinomas promote tumor growth and angiogenesis through elevated SDF-1/ CXCL12 secretion. *Cell* 2005;121:335–48.
18. De Wever O, Mareel M. Role of tissue stroma in cancer cell invasion. *J Pathol* 2003;200:429–47.
19. Lieubeau B, Garrigue L, Barbieux I, Meflah K, Gregoire M. The role of transforming growth factor beta 1 in the fibroblastic reaction associated with rat colorectal tumor development. *Cancer Res* 1994;54: 6526–32.
20. Hu M, Polyak K. Microenvironmental regulation of cancer development. *Curr Opin Genet Dev* 2008;18:27–34.
21. Hurst DR, Welch DR. A MSC-ing link in metastasis? *Nat Med* 2007;13:1289–91.
22. Paget S. The distribution of secondary growths in cancer of the breast. *Cancer Metastasis Rev* 1989;8:98–101.
23. Fidler IJ. Critical factors in the biology of human cancer metastasis: twenty-eighth G.H.A. Clowes memorial award lecture. *Cancer Res* 1990;50:6130–8.
24. Fidler IJ, Poste G. The cellular heterogeneity of malignant neoplasms: implications for adjuvant chemotherapy. *Semin Oncol* 1985;12:207–21.
25. Kitadai Y, Bucana CD, Ellis LM, Anzai H, Tahara E, Fidler IJ. In situ mRNA hybridization technique for analysis of metastasis-related genes in human colon carcinoma cells. *Am J Pathol* 1995;147: 1238–47.
26. Ishii M, Koike C, Igarashi A, Yamanaka K, Pan H, Higashi Y, Kawaguchi H, Sugiyama M, Kamata N, Iwata T, Matsubara T, Nakamura K, et al. Molecular markers distinguish bone marrow mesenchymal stem cells from fibroblasts. *Biochem Biophys Res Commun* 2005;332:297–303.
27. Tsutsumi S, Shimazu A, Miyazaki K, Pan H, Koike C, Yoshida E, Takagishi K, Kato Y. Retention of multilineage differentiation potential of mesenchymal cells during proliferation in response to FGF. *Biochem Biophys Res Commun* 2001;288:413–9.
28. Morikawa K, Walker SM, Jessup JM, Fidler IJ. In vivo selection of highly metastatic cells from surgical specimens of different primary human colon carcinomas implanted into nude mice. *Cancer Res* 1988;48:1943–8.
29. Morikawa K, Walker SM, Nakajima M, Pathak S, Jessup JM, Fidler IJ. Influence of organ environment on the growth, selection, and metastasis of human colon carcinoma cells in nude mice. *Cancer Res* 1988;48:6863–71.
30. Hwang RF, Yokoi K, Bucana CD, Tsan R, Killion JJ, Evans DB, Fidler IJ. Inhibition of platelet-derived growth factor receptor phosphorylation by STI571 (Gleevec) reduces growth and metastasis of human pancreatic carcinoma in an orthotopic nude mouse model. *Clin Cancer Res* 2003;9:6534–44.
31. Repesh LA. A new in vitro assay for quantitating tumor cell invasion. *Invasion Metastasis* 1989;9:192–208.
32. Studeny M, Marini FC, Champlin RE, Zompetta C, Fidler IJ, Andreeff M. Bone marrow-derived mesenchymal stem cells as vehicles for interferon-beta delivery into tumors. *Cancer Res* 2002;62:3603–8.
33. Chen X, Lin X, Zhao J, Shi W, Zhang H, Wang Y, Kan B, Du L, Wang B, Wei Y, Liu Y, Zhao X. A tumor-selective biotherapy with prolonged impact on established metastases based on cytokine gene-engineered MSCs. *Mol Ther* 2008;16:749–56.
34. Nakamizo A, Marini F, Amano T, Khan A, Studeny M, Gumin J, Chen J, Hentschel S, Vecil G, Dembinski J, Andreeff M, Lang FF. Human bone marrow-derived mesenchymal stem cells in the treatment of gliomas. *Cancer Res* 2005;65:3307–18.
35. Nakamura K, Ito Y, Kawano Y, Kurozumi K, Kobune M, Tsuda H, Bizen A, Honmou O, Niitsu Y, Hamada H. Antitumor effect of genetically engineered mesenchymal stem cells in a rat glioma model. *Gene Ther* 2004;11:1155–64.
36. Menon LG, Picinich S, Koneru R, Gao H, Lin SY, Koneru M, Mayer-Kuckuk P, Glod J, Banerjee D. Differential gene expression

associated with migration of mesenchymal stem cells to conditioned medium from tumor cells or bone marrow cells. *Stem Cells* 2007;25:520–8.
37. Beckermann BM, Kallifatidis G, Groth A, Frommhold D, Apel A, Mattern J, Salnikov AV, Moldenhauer G, Wagner W, Diehlmann A, Saffrich R, Schubert M, et al. VEGF expression by mesenchymal stem cells contributes to angiogenesis in pancreatic carcinoma. *Br J Cancer* 2008;99:622–31.
38. Kallifatidis G, Beckermann BM, Groth A, Schubert M, Apel A, Khamidjanov A, Ryschich E, Wenger T, Wagner W, Diehlmann A, Saffrich R, Krause U, et al. Improved lentiviral transduction of human mesenchymal stem cells for therapeutic intervention in pancreatic cancer. *Cancer Gene Ther* 2008;15:231–40.
39. Dwyer RM, Potter-Beirne SM, Harrington KA, Lowery AJ, Hennessy E, Murphy JM, Barry FP, O'Brien T, Kerin MJ. Monocyte chemotactic protein-1 secreted by primary breast tumors stimulates migration of mesenchymal stem cells. *Clin Cancer Res* 2007;13:5020–7.
40. Klopp AH, Spaeth EL, Dembinski JL, Woodward WA, Munshi A, Meyn RE, Cox JD, Andreeff M, Marini FC. Tumor irradiation increases the recruitment of circulating mesenchymal stem cells into the tumor microenvironment. *Cancer Res* 2007;67: 11687–95.
41. Fidler IJ, Wilmanns C, Staroselsky A, Radinsky R, Dong Z, Fan D. Modulation of tumor cell response to chemotherapy by the organ environment. *Cancer Metastasis Rev* 1994;13:209–22.
42. Weaver VM, Gilbert P. Watch thy neighbor: cancer is a communal affair. *J Cell Sci* 2004;117:1287–90.
43. Haviv I, Polyak K, Qiu W, Hu M, Campbell I. Origin of carcinoma associated fibroblasts. *Cell Cycle* 2009;8:589–95.
44. Spaeth EL, Dembinski JL, Sasser AK, Watson K, Klopp A, Hall B, Andreeff M, Marini F Mesenchymal stem cell transition to tumor-associated fibroblasts contributes to fibrovascular network expansion and tumor progression. *PLoS One* 2009;4:e4992.
45. Kalluri R, Zeisberg M. Fibroblasts in cancer. *Nat Rev Cancer* 2006;6:392–401.
46. Zeisberg EM, Potenta S, Xie L, Zeisberg M, Kalluri R. Discovery of endothelial to mesenchymal transition as a source for carcinoma-associated fibroblasts. *Cancer Res* 2007;67:10123–8.
47. Direkze NC, Hodivala-Dilke K, Jeffery R, Hunt T, Poulsom R, Oukrif D, Alison MR, Wright NA. Bone marrow contribution to tumor-associated myofibroblasts and fibroblasts. *Cancer Res* 2004;64:8492–5.

Journal of Pathology
J Pathol 2010; **221**: 275–284
Published online 7 May 2010 in Wiley InterScience
(www.interscience.wiley.com) DOI: 10.1002/path.2717

ORIGINAL PAPER

Search for transmembrane protein in gastric cancer by the *Escherichia coli* ampicillin secretion trap: expression of DSC2 in gastric cancer with intestinal phenotype

Katsuhiro Anami,[1] Naohide Oue,[1] Tsuyoshi Noguchi,[2] Naoya Sakamoto,[1] Kazuhiro Sentani,[1] Tetsutaro Hayashi,[1] Takao Hinoi,[3] Masazumi Okajima,[3] Jonathan M Graff[4] and Wataru Yasui[1]*

[1] *Department of Molecular Pathology, Hiroshima University Graduate School of Biomedical Sciences, Hiroshima, Japan*
[2] *Department of Gastrointestinal Surgery, Oita University Faculty of Medicine, Oita, Japan*
[3] *Department of Endoscopic Surgery and Surgical Science, Graduate School of Biomedical Science, Hiroshima University, Hiroshima, Japan*
[4] *Department of Developmental Biology, University of Texas Southwestern Medical Center, Dallas, Texas, USA*

**Correspondence to: Wataru Yasui, Department of Molecular Pathology, Hiroshima University Graduate School of Biomedical Sciences, 1-2-3 Kasumi, Minami-ku, Hiroshima 734-8551, Japan e-mail: wyasui@hiroshima-u.ac.jp*

Abstract

Gastric cancer (GC) is one of the most common malignancies worldwide. Genes expressed only in cancer tissue, and especially on the cell membrane, will be useful molecular markers for diagnosis and may also be good therapeutic targets. To identify genes that encode transmembrane proteins present in GC, we generated *Escherichia coli* ampicillin secretion trap (CAST) libraries from two GC cell lines and normal stomach. By sequencing 4320 colonies from CAST libraries, we identified 30 candidate genes that encode transmembrane proteins present in GC. Quantitative reverse transcription–polymerase chain reaction analysis of these candidates revealed that *ZDHHC14*, *BST2*, *DRAM2*, and *DSC2* were expressed much more highly in GC than in 14 kinds of normal tissues. Among these, *DSC2* encodes desmocollin 2, which is one of three known desmocollins. Immunohistochemical analysis demonstrated that 22 (28%) of 80 GC cases were positive for desmocollin 2, and desmocollin 2 expression was observed frequently in GC with the intestinal mucin phenotype. Furthermore, desmocollin 2 expression was correlated with CDX2 expression. These results suggest that expression of desmocollin 2, induced by CDX2, may be a key regulator for GC with the intestinal mucin phenotype. Our results provide a list of genes that have high potential as a diagnostic and therapeutic target for GC.

Keywords: CAST; gastric cancer; desmocollin 2; DSC2

Received 4 February 2010; Revised 9 March 2010; Accepted 29 March 2010

No conflicts of interest were declared.

Introduction

Gastric cancer (GC) is one of the most common human cancers. Cancer develops as a result of multiple genetic and epigenetic alterations [1]. Better knowledge of changes in gene expression that occur during gastric carcinogenesis may lead to improvements in diagnosis, treatment, and prevention. Identification of novel biomarkers for cancer diagnosis and novel targets for treatment is a major goal in this field [2]. Genes encoding transmembrane/secretory proteins expressed specifically in cancers may be ideal biomarkers for cancer diagnosis [3]. If the function of the gene product is involved in the neoplastic process, this gene may constitute a therapeutic target. We previously performed serial analysis of gene expression (SAGE) on four primary GC tissues [4] and identified several GC-specific genes [5]. Of these genes, *regenerating islet-derived family, member 4* (*REG4*, which encodes Reg IV) and *olfactomedin 4* (*OLFM4*, also known as GW112 or hGC-1) encode secreted proteins and serve as highly sensitive serum markers for GC [6,7]. However, through SAGE, we could not find GC-specific genes encoding transmembrane proteins.

In the present study, to identify genes that encode transmembrane proteins present in GC, we generated *Escherichia coli* ampicillin secretion trap (CAST) libraries from two GC cell lines, MKN-1 and MKN-28. CAST is a signal sequence trap method, developed by Ferguson *et al* [8]. Signal peptides target secreted and transmembrane proteins to their appropriate subcellular location, and typically consist of four to 15 hydrophobic amino acids flanked by a basic NH_2 terminus and a polar COOH terminus [9]. A consensus sequence for the signal peptide has not been identified and thus, standard molecular techniques are not well suited for identifying such proteins. CAST is a survival-based signal sequence trap method that exploits the ability of mammalian signal sequences to confer ampicillin

resistance to a mutant β-lactamase lacking the endogenous signal sequence [10]. We report here the identification of several genes that encode transmembrane proteins expressed in GC. Among these, we focused on the *DSC2* gene because this gene is frequently overexpressed in GC and *DSC2* expression is narrowly restricted in normal tissues. *DSC2* encodes desmocollin 2, which is one of the three known desmocollins. Desmocollins are membrane-spanning glycoproteins that form desmosomes along with desmogleins and function as Ca^{2+}-dependent cell adhesion molecules [11]. We examined the expression and distribution of desmocollin 2 in human GC by immunohistochemistry, and the relationship between desmocollin 2 staining and clinicopathological characteristics. Furthermore, because desmocollin 2 is expressed in intestinal metaplasia of the stomach, the association between desmocollin 2 expression and the mucin phenotype in GC was investigated.

Materials and methods

CAST library construction

CAST library construction was performed as described previously [8].

Tissue samples

In total, 457 primary tumour samples were collected from patients diagnosed with GC. Patients were treated at the Hiroshima University Hospital or an affiliated hospital. Because written informed consent was not obtained, for strict privacy protection, identifying information for all samples was removed before analysis. This procedure was in accordance with the Ethical Guidelines for Human Genome/Gene Research of the Japanese Government.

For quantitative reverse transcription-polymerase chain (RT-PCR) reaction, 50 GC samples and corresponding non-neoplastic mucosa samples were used. Samples were frozen immediately in liquid nitrogen and stored at −80 °C until use. Non-cancerous samples of heart, lung, stomach, small intestine, colon, liver, pancreas, kidney, bone marrow, peripheral leukocytes, spleen, skeletal muscle, brain, and spinal cord were purchased from Clontech (Palo Alto, CA, USA).

For immunohistochemical analysis, we used archival formalin-fixed, paraffin-embedded tissues from 407 patients who had undergone surgical excision for GC. Of 407 GC samples, one or two representative tumour blocks were examined from each patient by immunohistochemistry in 80 GC samples. Immunohistochemical analysis of the remaining 327 GC samples was carried out in a tissue microarray (TMA) [12]. Tumour staging was according to the TNM classification system [13]. Histological classification of GC was carried out according to the Lauren classification system [14].

Quantitative RT-PCR and western blot

Quantitative RT-PCR was performed with an ABI PRISM 7700 Sequence Detection System (Applied Biosystems, Foster City, CA, USA) as described previously [15]. Western blot was performed as described previously [16]. Detailed information of quantitative RT-PCR and western blot is described in the Supporting information, Supplementary material.

Evaluation of the specificity of gene expression

To evaluate the specificity of expression of each gene, a specificity index was calculated as follows: first, we identified the normal tissue in which the target gene expression was highest among the 14 normal tissues analysed by quantitative RT-PCR (the mRNA expression level in this tissue was denoted as A). We then identified GC among the nine GC samples in which the target gene expression was highest by quantitative RT-PCR (the mRNA expression level in this tissue was denoted as B). The ratio B to A was defined as the specificity index. When the specificity index of the target gene was greater than or equal to 10, the gene was considered to show high specificity for GC. When the specificity index of the target gene was less than 10 and greater than or equal to 2, the gene was considered to show low specificity for GC. When the specificity index of the target gene was less than 2, the gene was considered to show no specificity for GC.

Immunohistochemistry

Immunohistochemical analysis was performed with a Dako Envision + Mouse Peroxidase Detection System (Dako Cytomation, Carpinteria, CA, USA). Antigen retrieval was done by heating in citrate buffer (pH 6.0) in a microwave oven for 30 min. After peroxidase activity was blocked with 3% H_2O_2–methanol for 10 min, sections were incubated with normal goat serum (Dako Cytomation) for 20 min to block non-specific antibody binding sites. Sections were incubated with the following antibody dilutions: mouse monoclonal anti-desmocollin 2 (LifeSpan BioSciences, Inc, Seattle, WA, USA), 1 : 50, and mouse monoclonal anti-CDX2, 1 : 50 (BioGenex, San Ramon, CA, USA). Sections were incubated with primary antibody for 1 h at room temperature, followed by incubations with Envision+ anti-mouse peroxidase for 1 h. For colour reaction, except for the normal heart, sections were incubated with the DAB Substrate-Chromogen Solution (Dako Cytomation) for 10 min. For colour reaction of the normal heart, sections were incubated with the AEC Substrate-Chromogen Solution (Dako Cytomation) for 10 min. Sections were counterstained with 0.1% haematoxylin. A result was considered positive if at least 10% of the cells were stained. When fewer than 10% of cancer cells were stained, the immunostaining was considered negative.

Phenotypic analysis of GC

GCs were classified into four phenotypes: gastric (G) type, intestinal (I) type, gastric and intestinal mixed (GI) type, and unclassified (N) type. For phenotypic expression analysis of GC, we performed immunohistochemical analysis (as described above) with four antibodies: anti-MUC5AC (Novocastra, Newcastle, UK) as a marker of foveolar epithelial cells in the stomach; anti-MUC6 (Novocastra) as a marker of pyloric gland cells in the stomach; anti-MUC2 (Novocastra) as a marker of goblet cells in the small intestine and colorectum; and anti-CD10 (Novocastra) as a marker of microvilli of absorptive cells in the small intestine and colorectum. The criteria [17] for the classification of G-type and I-type GCs were as follows: GCs in which more than 10% of cells in the section expressed at least one gastric epithelial cell marker (MUC5AC or MUC6) or intestinal epithelial cell marker (MUC2 or CD10) were classified as G-type or I-type cancers, respectively. Sections that showed both gastric and intestinal phenotypes were classified as GI type, and those that lacked both the gastric and the intestinal phenotypes were classified as N type.

Cell lines

Eight cell lines derived from human GC were used. Detailed information of the GC cell lines is described in the Supporting information, Supplementary material. To assess *DSC2* as a CDX2-regulated gene, the HT-29 cell line was inoculated with the pCDX2-ER vector as described previously [18]. The pCDX2-ER vector encodes a chimeric protein in which full-length CDX2 sequences are fused upstream of a mutated oestrogen receptor (ER) ligand-binding domain. The mutated ER ligand-binding domain no longer binds oestrogen, but retains the ability to bind tamoxifen. In HT-29 cells expressing the CDX2–ER fusion protein (HT-29/CDX2-ER), CDX2 function was activated by the addition of 4-hydroxytamoxifen (4-OHT) (Sigma Chemical, St Louis, MO, USA) to the growth medium at a final concentration of 500 nmol/l.

RNA interference (RNAi) and cell growth and *in vitro* invasion assays

To knockdown the endogenous *DSC2*, RNAi was performed. Short interfering RNA (siRNA) oligonucleotides for *DSC2* and a negative control were purchased from Invitrogen (Carlsbad, CA, USA). 3-(4,5-Dimethylthiazol-2-yl)-2,5-diphenyltetrazolium bromide (MTT) [19] and modified Boyden chamber assays were performed to examine cell growth and invasiveness, respectively (see Supporting information, Supplementary material).

Statistical method

Correlations between clinicopathological parameters and desmocollin 2 protein expression were analysed by Fisher's exact test. A p value of less than 0.05 was considered statistically significant.

Results

Generation of CAST libraries

To identify genes that encode transmembrane proteins present in GC, we generated CAST libraries from two GC cell lines (MKN-1 and MKN-28) and normal stomach. We sequenced 1440 ampicillin-resistant colonies from each CAST library. We compared these sequences with those deposited in the public databases using BLAST (accessed at http://blast.ncbi.nlm.nih.gov/Blast.cgi) and evaluated the subcellular localization of the gene products using data from GeneCards (accessed at http://www.genecards.org/index.shtml). Of 1440 colonies from the MKN-1 cell line, 1035 colonies were human named genes, which included 359 genes. In order for the *E. coli* to survive the antibiotic challenge, the signal sequence and translation initiator ATG codon must be cloned in-frame with the leaderless β-lactamase reporter. Among the 359 genes, 152 genes were cloned in-frame upstream of the leaderless β-lactamase gene. Of the 152 genes, ten genes encoded secreted proteins; 58 genes encoded transmembrane proteins; and 76 genes encoded proteins that were not secreted proteins or transmembrane proteins. The remaining eight genes were not well studied. Of 1440 colonies from the MKN-28 cell line, 1173 colonies expressed human named genes, which included 313 genes. Among the 313 genes, 154 genes were cloned in-frame upstream of the leaderless β-lactamase gene. Of these 154 genes, 13 genes encoded secreted proteins; 59 genes encoded transmembrane proteins; and 74 genes encoded proteins that were not secreted proteins or transmembrane proteins. The remaining eight genes were not well studied. Of 1440 colonies from normal stomach, 1248 colonies were human named genes, which included 158 genes. Among the 158 genes, 77 genes were cloned in-frame upstream of the leaderless β-lactamase gene. Of these 77 genes, 11 genes encoded secreted proteins; 29 genes encoded transmembrane proteins; and 30 genes encoded proteins that were not secreted proteins or transmembrane proteins. The remaining seven genes were not well studied. Because the purpose of this study was to identify genes that encode transmembrane proteins present in GC, we focused on transmembrane proteins.

Identification of genes expressed more highly in GC than in normal tissues

To identify genes expressed specifically in GC, we compared the gene list from each GC cell line CAST library with the normal stomach CAST library. We selected only genes that were detected at least twice

Table 1. Summary of quantitative RT-PCR analysis of candidate genes specifically expressed in gastric cancer

Gene name	Normal organ with highest expression: Organ name	Normal organ with highest expression: mRNA expression level (A)	GC with highest expression mRNA expression level (B)	Specificity index (B/A)	Number of GC cases with mRNA expression level 2-fold greater than normal organ with highest expression	Number of GC cases with mRNA expression level 10-fold greater than normal organ with highest expression
High specificity						
PCDHB9	Skeletal muscle	2.9*	576*	198.6	7	4
C4orf34	Pancreas	6.6	418.8	63.5	2	1
ADAM17	Small intestine	3.6	187.4	52.1	3	1
TMEM50B	Pancreas	3	97	32.3	5	2
ENPP4	Leukocyte	4.9	96.3	19.7	1	1
SLC38A2	Skeletal muscle	16.2	162.6	10	2	0
Low specificity						
CD151	Small intestine	25.1	191.3	7.6	1	0
RFT1	Pancreas	11.6	78.8	6.8	2	0
CLDN7	Colon	28.9	150.2	5.2	2	0
DSC2	Heart	12.7	40.8	3.2	1	0
BST2	Liver	16.2	50.2	3.1	2	0
ZDHHC14	Brain	8.9	23.6	2.7	1	0
APP	Small intestine	21.1	56.5	2.7	1	0
DRAM2	Heart	2.3	5.8	2.5	1	0
No specificity						
ATP13A3	Heart	6.5	10.6	1.6	0	0
SLC12A2	Colon	1.2	1.8	1.5	0	0
AGPAT5	Pancreas	10	13.7	1.4	0	0
SLC7A1	Pancreas	19.6	28.2	1.4	0	0
ATP8B1	Pancreas	3.7	3.7	1	0	0
LNPEP	Skeletal muscle	4.7	4.3	0.9	0	0
PTP4A1	Skeletal muscle	29.9	24.1	0.8	0	0
XPR1	Heart	20.4	16.4	0.8	0	0
CD63	Pancreas	6.6	4.6	0.7	0	0
TFRC	Heart	15.3	10.9	0.7	0	0
SLC35F5	Skeletal muscle	9.1	5.1	0.6	0	0
SLC38A9	Pancreas	11.3	6.4	0.6	0	0
TM9SF4	Pancreas	13.1	7.6	0.6	0	0
C3orf1	Heart	32.4	12.9	0.4	0	0
SLC44A2	Skeletal muscle	112.2	42.2	0.4	0	0
TM7SF3	Kidney	9.3	2.1	0.2	0	0

*The units are arbitrary. Target mRNA expression levels were standardized to 1.0 μg total RNA from normal stomach as 1.0.

in each GC cell line CAST library. In addition, genes were selected that were not found in the normal stomach CAST library. We obtained 19 candidates from MKN-1 and 17 candidates from MKN-28. In total, 30 individual candidate genes were identified (Table 1). To confirm that these candidates were GC-specific, quantitative RT-PCR was performed to measure the expression of these candidates in nine GC tissue samples and in 14 normal tissues. Representative results are shown in Figure 1. Expression of the 30 candidate genes was not necessarily specific for GC. However, several genes showed much higher expression in GC than in normal tissues. We then focused on cancer specificity by calculating the specificity index for each gene. First, we identified the normal tissue in which the target gene expression was highest (mRNA expression levels are shown as A, Table 1). We then identified the GC among nine tissues in which the target gene expression was highest (mRNA expression levels are shown as B, Table 1). The specificity index (B/A ratio) for each gene is shown in Table 1. Of the 30 candidates, six genes—*PCDHB9, C4orf34, ADAM17, TMEM50B, ENPP4*, and *SLC38A2*—were found to show high specificity for GC, and eight genes—*CD151, RFT1, CLDN7, DSC2, BST2, ZDHHC14, APP*, and *DRAM2*—were found to show low specificity for GC.

mRNA expression of high- and low-specificity genes for GC

Expression of the six high-specificity and eight low-specificity genes for GC was analysed by quantitative RT-PCR in an additional 41 GC samples and corresponding non-neoplastic mucosa samples. We calculated the ratio of target gene mRNA expression levels between GC tissue (T) and corresponding non-neoplastic mucosa (N). T/N ratios greater than two-fold were considered to represent overexpression. Genes showing overexpression in more than 30% of the samples included *ZDHHC14* (19/41, 46%), *BST2* (16/41, 39%), *DRAM2* (15/41, 37%), and *DSC2* (13/41, 32%).

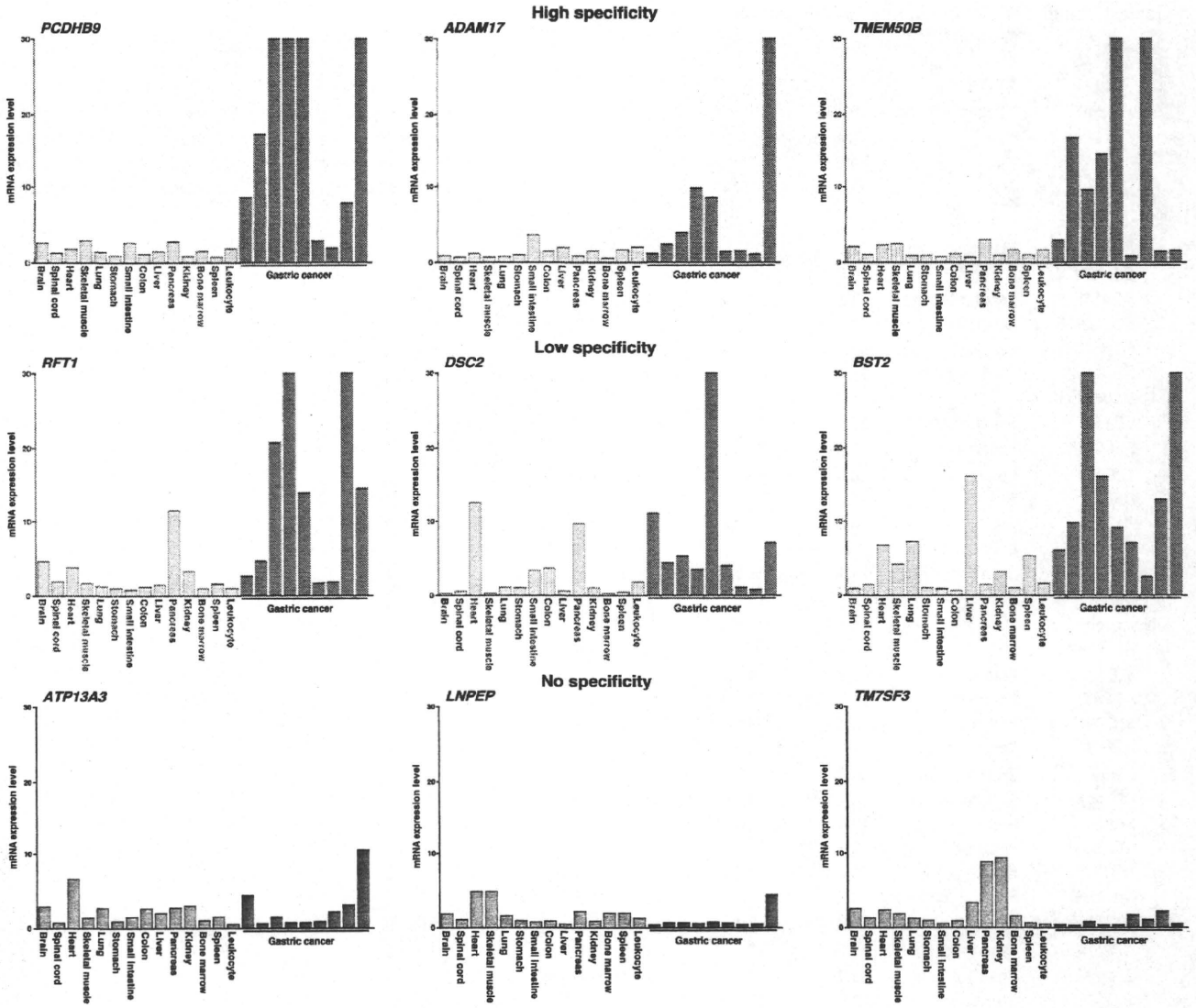

Figure 1. Quantitative RT-PCR analysis of candidate genes that encode cell surface proteins in 14 normal tissues and nine GC samples. Definitions of high specificity, low specificity, and no specificity are described in the Materials and methods section. mRNA expression levels of *PCDHB9*, *ADAM17*, and *TMEM50B* were much higher in GC samples than in normal tissues. In contrast, mRNA expression levels of *ATP13A3*, *LNPEP*, and *TM7SF3* were not significantly different between GC and normal tissues.

Other genes were overexpressed in less than 30% of the samples examined (*RFT1*, 10/41, 24%; *PCDHB9*, 8/41, 20%; *TMEM50B*, 8/41, 20%; *C4orf34*, 6/41, 15%; and *SLC38A2*, 5/41, 12%).

Immunohistochemical staining for DSC2 in GC and non-cancerous tissues

To confirm overexpression of genes whose expression by quantitative RT-PCR was much higher in GC than in normal tissues, we performed immunohistochemical analysis. Among four genes that were frequently overexpressed in GC, we focused on *DSC2* because an antibody against DSC2 protein is commercially available. *DSC2* encodes desmocollin 2, and desmocollins are membrane-spanning glycoproteins that function as Ca^{2+}-dependent cell adhesion molecules [11]. Although desmocollin 2 is expressed in normal colonic epithelium, its expression is reduced in colorectal cancer [20]. There are no reports of desmocollin 2 expression in GC. Immunohistochemical analysis was first performed in non-cancerous tissues with the obvious mRNA expression to serve as positive controls. Immunostaining of desmocollin 2 in the normal heart showed staining of cardiomyocytes (Figure 2A). Immunostaining in the normal pancreas revealed that duct epithelial cells expressed desmocollin 2 on cell membranes (Figure 2B). As reported previously, colonic epithelial cells expressed desmocollin 2 on cell membranes (Figure 2C). These results are consistent with our quantitative RT-PCR results.

Next, immunohistochemistry was performed on 80 GC samples. In non-neoplastic gastric mucosa, weak or no staining of desmocollin 2 was observed in the foveolar epithelium, whereas desmocollin 2 was expressed in the intestinal metaplasia (Figure 2D). Expression of desmocollin 2 was not detected in stromal cells, such as inflammatory cells and fibroblasts. In contrast, GC tissue showed stronger, more extensive

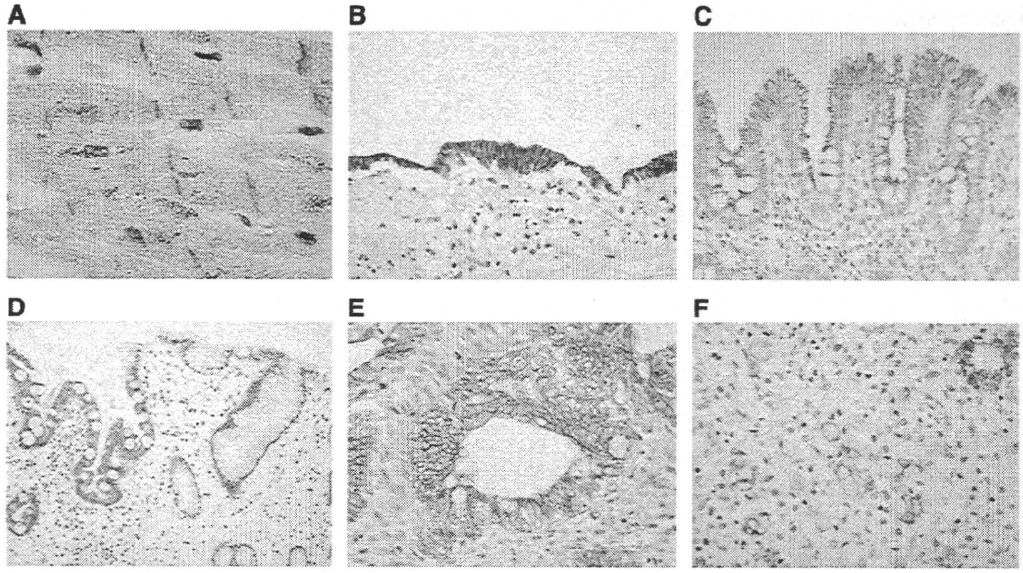

Figure 2. Immunohistochemical analysis of desmocollin 2 in non-neoplastic human tissues and GC tissues. (A) Immunostaining of desmocollin 2 in the normal heart showed staining of cardiomyocytes. Note that the signal is red (using AEC Substrate-Chromogen Solution) to differentiate the staining from the brown pigment in cardiomyocytes. Original magnification: 1000×. (B) Immunostaining of desmocollin 2 in non-neoplastic pancreas revealed that duct epithelial cells expressed desmocollin 2 on cell membranes. Original magnification: 400×. (C) Immunostaining of desmocollin 2 in non-neoplastic colon revealed that colonic epithelial cells expressed desmocollin 2 on cell membranes. Original magnification: 400×. (D) Immunostaining of desmocollin 2 in non-neoplastic gastric mucosa. Desmocollin 2 was present in intestinal metaplasia. Original magnification: 200×. (E) Immunostaining of desmocollin 2 in intestinal-type GC. Desmocollin 2 staining was observed in GC cells on cell membranes. Original magnification: 400×. (F) Immunostaining of desmocollin 2 in diffuse-type GC. Desmocollin 2 staining was observed in GC cells on cell membranes. Original magnification: 400×.

staining than corresponding non-neoplastic mucosa. Desmocollin 2 staining was frequently observed in intestinal-type GC (Figure 2E). Most diffuse-type GCs did not express desmocollin 2; however, some signet ring cell carcinoma cells did stain for desmocollin 2 (Figure 2F). Some GCs showed heterogeneity of desmocollin 2 immunostaining and the percentage of desmocollin 2-positive tumour cells ranged from 0% to 80%. The relationship of desmocollin 2 staining to clinicopathological characteristics was investigated (Table 2). When at least 10% of tumour cells were stained, the immunostaining was considered positive for desmocollin 2. In total, 22 (28%) of 80 GC cases were positive for desmocollin 2. Desmocollin 2 staining was observed more frequently in stage I/II cases (16/41, 39%) than in stage III/IV cases (6/39, 15%, $p = 0.0243$, Fisher's exact test). Moreover, desmocollin 2 staining was detected more frequently in intestinal-type GC (20/46, 46%) than in diffuse-type GC (2/34, 6%, $p < 0.0001$, Fisher's exact test). In the group of 59 advanced GC patients, no statistically significant prognostic impact was found (data not shown).

Desmocollin 2 is expressed in GC with the intestinal phenotype

Despite the usefulness of the Lauren classification, it was previously reported that GC can be subdivided into four phenotypes according to mucin expression (G type, I type, GI type, and N type) [21]. We further investigated the association between desmocollin 2 expression and the mucin phenotype, because desmocollin 2 was detected in intestinal metaplasia of the stomach and colon. Immunohistochemical analysis of gastric (MUC5AC and MUC6) and intestinal (MUC2 and CD10) markers was carried out in a TMA of 327 GC cases. In general, desmocollin 2 was frequently expressed in MUC2-positive GC cases (Figure 3A). Desmocollin 2 staining was detected more frequently in MUC2-positive GC (33/61, 54%) than in MUC2-negative GC (74/266, 28%, $p < 0.0001$, Fisher's exact test). However, desmocollin 2 was also expressed in tumour cells that did not express MUC2. There was no clear relationship between expression of desmocollin 2 and MUC5AC, MUC6, or CD10. On the basis of the expression of these four markers, we classified the 327 GC cases phenotypically as 133 (40%) G type, 55 (17%) I type, 64 (20%) GI type, and 75 (23%) N type. Expression of desmocollin 2 was observed more frequently in I-type GC than in other (G, GI, and N) GC types ($p = 0.0396$, Fisher's exact test) (Figure 3B).

CDX2 induces desmocollin 2 expression

We found that expression of desmocollin 2 is associated with the intestinal mucin phenotype in GC. It is known that intestinal metaplasia of the stomach and GC with the intestinal mucin phenotype are associated with ectopic CDX2 expression [21,22]. It has been reported that CDX2 interacts with the *DSC2* promoter and activates *DSC2* transcription [23]. To confirm the relationship between CDX2 function and *DSC2* gene expression, we studied desmocollin 2 expression in

Table 2. Relationship between desmocollin 2 expression and clinicopathological characteristics in gastric cancer

	Desmocollin 2 expression		
	Positive	Negative	*p* value*
Age, years			
≤65	6 (29%)	15	1.0000
>65	16 (27%)	43	
Sex			
Male	14 (26%)	39	0.7951
Female	8 (30%)	19	
T classification†			
T1	8 (38%)	13	0.2574
T2/3/4	14 (24%)	45	
N classification‡			
N0	10 (31%)	22	0.6130
N1/2/3	12 (25%)	36	
Stage			
I/II	16 (39%)	25	0.0243
III/IV	6 (15%)	33	
Histological classification			
Intestinal	20 (43%)	26	<0.0001
Diffuse	2 (6%)	32	

*Fisher's exact test. †T1, tumour invades lamina propria or submucosa; T2, tumour invades muscularis propria or subserosa; T3, tumour penetrates serosa; T4, tumour invades adjacent structures. ‡N0, no regional lymph node metastasis; N1, metastasis in one to six regional lymph nodes; N2, metastasis in seven to 15 regional lymph nodes; N3, metastasis in more than 15 regional lymph nodes.

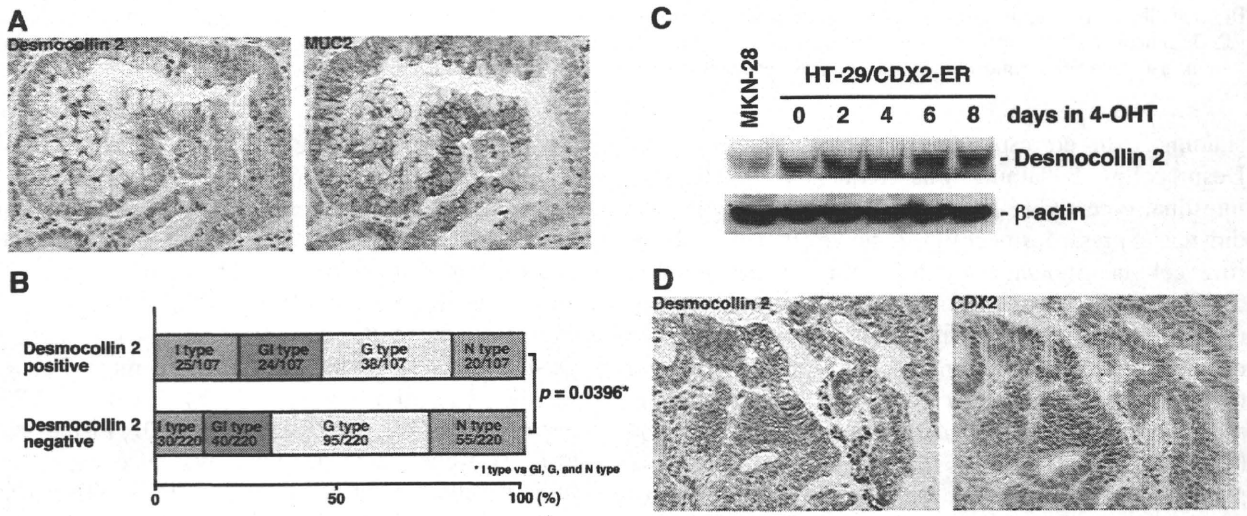

Figure 3. Expression of the mucin phenotype of GC. (A) Expression of desmocollin 2 and MUC2 in GC. In this case, desmocollin 2 was detected in GC cell membranes. MUC2 was also expressed, but several desmocollin 2-positive GC cells did not express MUC2. Original magnification: 400×. (B) Summary of desmocollin 2 expression and expression of the mucin phenotype. Desmocollin 2-positive GC cases were found more frequently in I-type GC than in the other (GI, G, and N) GC types. *Fisher's exact test. (C) Western blot analysis of desmocollin 2. Time course of desmocollin 2 induction in response to activation of a CDX2–ER fusion protein by 4-OHT. (D) Expression of desmocollin 2 and CDX2 in GC. Original magnification: 400×.

an HT-29-derived line with tightly regulated CDX2 activity [18,24]. We used a polyclonal HT-29 cell line that had been transduced with a vector encoding a chimeric CDX2–ER fusion protein. Treatment of the HT-29/CDX2-ER cell line with 4-OHT resulted in strong induction of desmocollin 2 protein expression within 2 days (Figure 3C). These results indicate that *DSC2* is a direct or primary target gene regulated by CDX2.

We then investigated whether CDX2 induces desmocollin 2 expression in GC tissue. Immunohistochemical analysis of CDX2 was carried out in a TMA (Figure 3D). Of 327 GC cases, 74 (23%) GC cases were positive for CDX2. Desmocollin 2 staining was found more frequently in CDX2-positive GC (44/74, 59%) than in CDX2-negative GC (63/253, 25%, $p < 0.0001$, Fisher's exact test). However, desmocollin 2 was also stained in tumour cells that were negative for CDX2.

Effect of desmocollin 2 inhibition on cell growth and invasive activity

Desmocollin 2-positive GC cases were observed more frequently in stage I/II than in stage III/IV, suggesting that desmocollin 2 may be associated with tumour progression; however, the biological significance of

desmocollin 2 in human cancer has not been studied. To investigate the possible anti-proliferative effect of desmocollin 2 knockdown, we performed an MTT assay 8 days after siRNA transfection in the MKN-1, MKN-28, and MKN-45 cell lines; however, cell viability was not significantly different between desmocollin 2 siRNA-transfected GC cells and negative control siRNA-transfected GC cells (data not shown). Next, to determine the possible role of desmocollin 2 in the invasiveness of GC cells, a transwell invasion assay was performed in the MKN-1, MKN-28, and MKN-45 cell lines. Invasion ability was not significantly different between desmocollin 2 knockdown GC cells and negative control siRNA-transfected GC cells (data not shown).

Discussion

In the present study, we generated CAST libraries from two GC cell lines and identified several genes that encode transmembrane proteins present in GC. Quantitative RT-PCR revealed that *PCDHB9, C4orf34, ADAM17, TMEM50B, ENPP4, SLC38A2, CD151, RFT1, CLDN7, DSC2, BST2, ZDHHC14, APP*, and *DRAM2* were expressed much more highly in GC than in 14 types of normal tissues. Quantitative RT-PCR in an additional 41 GC samples revealed that *ZDHHC14, BST2, DRAM2*, and *DSC2* were overexpressed in more than 30% of the samples. Because these genes were identified by CAST analysis of GC cell lines and quantitative RT-PCR analysis of bulk GC tissues, immunohistochemistry was required to determine which cells expressed these genes. Among these four genes, only an antibody against desmocollin 2 was commercially available. Therefore, we performed immunohistochemical analysis of desmocollin 2 in GC and found that 22 (28%) of 80 GC cases were positive for desmocollin 2. Desmocollin 2 was frequently expressed in MUC2-positive GC cases, and desmocollin 2 expression was observed frequently in I-type GC. Ectopic CDX2 expression plays an important role in the development of I-type GC [21,22] and it has been reported that CDX2 activates *DSC2* transcription [23]. In the present study, we showed that desmocollin 2 expression was correlated with CDX2 expression in GC tissue. Taken together, expression of desmocollin 2, induced by CDX2, may be a key factor mediating the biological behaviour of I-type GC.

In quantitative RT-PCR, *DSC2* was overexpressed in 32% of the samples examined. The observation is based on a comparison of GC with corresponding non-neoplastic mucosa. I-type GC contains I-type GC cells, whereas corresponding non-neoplastic mucosa is composed of a mixed population of foveolar, oxyntic, and endocrine cells. Because *DSC2*, similar to *CDX2*, is a marker of the intestinal mucin phenotype in both normal and GC cells, it is not surprising that *DSC2* is enriched in GC when compared with corresponding non-neoplastic mucosa containing foveolar epithelium. Therefore, it is correct to say that *DSC2* is ectopically expressed in GC, rather than overexpressed in GC.

In immunohistochemical analysis, desmocollin 2 is variably expressed in the normal upper gastrointestinal tract and thus, desmocollin 2 expression in I-type GC is not specific. Knockdown of desmocollin 2 by RNAi did not affect cell growth and invasiveness in GC cell lines. These results indicate that desmocollin 2 expression is not likely to be involved in carcinogenesis. Because desmocollin 2 is a membrane-spanning glycoprotein that functions as a Ca^{2+}-dependent cell adhesion molecule, there is a possibility that desmocollin 2 plays an important role in glandular formation of GC cells. In the present study, desmocollin 2 staining was observed more frequently in stage I/II cases than in stage III/IV cases. Therefore, loss of desmocollin 2 expression may be associated with tumour progression.

Several lines of evidence suggest that distinct cell surface or cell adhesion molecules are expressed in G-type GC and I-type GC. The claudin protein family, which comprises 24 members, is a component of tight junctions. All claudins are 20–27 kDa proteins with four transmembrane domains [25]. Expression of claudin-18 is frequently down-regulated in I-type GC [26]. In contrast, ectopic expression of claudin-3 and claudin-4 is found in I-type GC [27]. Liver-intestine cadherin (LI-cadherin), which is a member of the cadherin family of cell adhesion molecules [28], is one of the CDX2-regulated genes [18]. Ectopic expression of LI-cadherin is observed in I-type GC [29]. Taken together with the present results, it seems that the biological characteristics of I-type GC are different from those of G-type GC and thus, classification of GC based on the mucin phenotype is important for treatment of GC. In fact, distinctive responses to chemotherapy between G-type and I-type GC have been reported [30].

In summary, our present study yielded a list of genes that encode transmembrane proteins present in GC. We found that desmocollin 2 is expressed in GC and that expression of desmocollin 2 is associated with the intestinal mucin phenotype. We identified several genes by quantitative RT-PCR that have not been implicated previously in GC. Our current data also provide information with respect to the expression of these genes throughout the body. Additional examination including functional and immunohistochemical analysis will certify whether the genes identified in the present study may constitute not only a diagnostic but also a therapeutic target.

Acknowledgment

We thank Mr Shinichi Norimura for his excellent technical assistance and advice. This work was carried out with the kind cooperation of the Research Center for

Molecular Medicine, Faculty of Medicine, Hiroshima University. We thank the Analysis Center of Life Science, Hiroshima University for the use of their facilities. This work was supported in part by Grants-in-Aid for Cancer Research from the Ministry of Education, Culture, Science, Sports, and Technology of Japan; in part by a Grant-in-Aid for the Third Comprehensive 10-Year Strategy for Cancer Control and for Cancer Research from the Ministry of Health, Labour, and Welfare of Japan; and in part by a grant (07-23911) from the Princess Takamatsu Cancer Research Fund.

References

Note: References 31–33 are cited in the Supporting information to this article.

1. Yasui W, Oue N, Kitadai Y, Nakayama H. Recent advances in molecular pathobiology of gastric carcinoma. In *The Diversity of Gastric Carcinoma Pathogenesis: Diagnosis and Therapy*, Kaminishi M, Takubo K, Mafune K (eds). Springer: Tokyo, 2005; 51–71.
2. Yasui W, Oue N, Ito R, Kuraoka K, Nakayama H. Search for new biomarkers of gastric cancer through serial analysis of gene expression and its clinical implications. *Cancer Sci* 2004; **95**: 385–392.
3. Buckhaults P, Rago C, St Croix B, Romans KE, Saha S, Zhang L, *et al*. Secreted and cell surface genes expressed in benign and malignant colorectal tumors. *Cancer Res* 2001; **61**: 6996–7001.
4. Oue N, Hamai Y, Mitani Y, Matsumura S, Oshimo Y, Aung PP, *et al*. Gene expression profile of gastric carcinoma: identification of genes and tags potentially involved in invasion, metastasis, and carcinogenesis by serial analysis of gene expression. *Cancer Res* 2004; **64**: 2397–2405.
5. Aung PP, Oue N, Mitani Y, Nakayama H, Yoshida K, Noguchi T, *et al*. Systematic search for gastric cancer-specific genes based on SAGE data: melanoma inhibitory activity and matrix metalloproteinase-10 are novel prognostic factors in patients with gastric cancer. *Oncogene* 2006; **25**: 2546–2557.
6. Mitani Y, Oue N, Matsumura S, Yoshida K, Noguchi T, Ito M, *et al*. Reg IV is a serum biomarker for gastric cancer patients and predicts response to 5-fluorouracil-based chemotherapy. *Oncogene* 2007; **26**: 4383–4393.
7. Oue N, Sentani K, Noguchi T, Ohara S, Sakamoto N, Hayashi T, *et al*. Serum olfactomedin 4 (GW112, hGC-1) in combination with Reg IV is a highly sensitive biomarker for gastric cancer patients. *Int J Cancer* 2009; **125**: 2383–2392.
8. Ferguson DA, Muenster MR, Zang Q, Spencer JA, Schageman JJ, Lian Y, *et al*. Selective identification of secreted and transmembrane breast cancer markers using *Escherichia coli* ampicillin secretion trap. *Cancer Res* 2005; **65**: 8209–8217.
9. von Heijne G. A new method for predicting signal sequence cleavage sites. *Nucleic Acids Res* 1986; **14**: 4683–4690.
10. Kadonaga JT, Gautier AE, Straus DR, Charles AD, Edge MD, Knowles JR. The role of the beta-lactamase signal sequence in the secretion of proteins by *Escherichia coli*. *J Biol Chem* 1984; **259**: 2149–2154.
11. Yin T, Green KJ. Regulation of desmosome assembly and adhesion. *Semin Cell Dev Biol* 2004; **15**: 665–677.
12. Sentani K, Oue N, Noguchi T, Sakamoto N, Matsusaki K, Yasui W. Immunostaining of gastric cancer with neuroendocrine differentiation: Reg IV-positive neuroendocrine cells are associated with gastrin, serotonin, pancreatic polypeptide and somatostatin. *Pathol Int* (in press).
13. Sobin LH, Wittekind CH (eds). *TNM Classification of Malignant Tumors* (6th edn). Wiley-Liss: New York, 2002; 65–68.
14. Lauren P. The two histological main types of gastric carcinoma: diffuse and so-called intestinal-type carcinoma. An attempt at a histo-clinical classification. *Acta Pathol Microbiol Scand* 1965; **64**: 31–49.
15. Kondo T, Oue N, Yoshida K, Mitani Y, Naka K, Nakayama H, *et al*. Expression of POT1 is associated with tumor stage and telomere length in gastric carcinoma. *Cancer Res* 2004; **64**: 523–529.
16. Yasui W, Ayhan A, Kitadai Y, Nishimura K, Yokozaki H, Ito H, *et al*. Increased expression of p34cdc2 and its kinase activity in human gastric and colonic carcinomas. *Int J Cancer* 1993; **53**: 36–41.
17. Mizoshita T, Tsukamoto T, Nakanishi H, Inada K, Ogasawara N, Joh T, *et al*. Expression of Cdx2 and the phenotype of advanced gastric cancers: relationship with prognosis. *J Cancer Res Clin Oncol* 2003; **129**: 727–734.
18. Hinoi T, Lucas PC, Kuick R, Hanash S, Cho KR, Fearon ER. CDX2 regulates liver intestine-cadherin expression in normal and malignant colon epithelium and intestinal metaplasia. *Gastroenterology* 2002; **123**: 1565–1577.
19. Alley MC, Scudiero DA, Monks A, Hursey ML, Czerwinski MJ, Fine DL, *et al*. Feasibility of drug screening with panels of human tumor cell lines using a microculture tetrazolium assay. *Cancer Res* 1988; **48**: 589–601.
20. Khan K, Hardy R, Haq A, Ogunbiyi O, Morton D, Chidgey M. Desmocollin switching in colorectal cancer. *Br J Cancer* 2006; **95**: 1367–1370.
21. Tatematsu M, Tsukamoto T, Inada K. Stem cells and gastric cancer: role of gastric and intestinal mixed intestinal metaplasia. *Cancer Sci* 2003; **94**: 135–141.
22. Silberg DG, Sullivan J, Kang E, Swain GP, Moffett J, Sund NJ, *et al*. Cdx2 ectopic expression induces gastric intestinal metaplasia in transgenic mice. *Gastroenterology* 2002; **122**: 689–696.
23. Funakoshi S, Ezaki T, Kong J, Guo RJ, Lynch JP. Repression of the desmocollin 2 gene expression in human colon cancer cells is relieved by the homeodomain transcription factors Cdx1 and Cdx2. *Mol Cancer Res* 2008; **6**: 1478–1490.
24. Hinoi T, Gesina G, Akyol A, Kuick R, Hanash S, Giordano TJ, *et al*. CDX2-regulated expression of iron transport protein hephaestin in intestinal and colonic epithelium. *Gastroenterology* 2005; **128**: 946–961.
25. Tsukita S, Furuse M, Itoh M. Multifunctional strands in tight junctions. *Nature Rev Mol Cell Biol* 2001; **2**: 285–293.
26. Sanada Y, Oue N, Mitani Y, Yoshida K, Nakayama H, Yasui W. Down-regulation of the claudin-18 gene, identified through serial analysis of gene expression data analysis, in gastric cancer with an intestinal phenotype. *J Pathol* 2006; **208**: 633–642.
27. Matsuda Y, Semba S, Ueda J, Fuku T, Hasuo T, Chiba H, *et al*. Gastric and intestinal claudin expression at the invasive front of gastric carcinoma. *Cancer Sci* 2007; **98**: 1014–1019.
28. Berndorff D, Gessner R, Kreft B, Schnoy N, Lajous-Petter AM, Loch N, *et al*. Liver-intestine cadherin: molecular cloning and characterization of a novel Ca(2+)-dependent cell adhesion molecule expressed in liver and intestine. *J Cell Biol* 1994; **125**: 1353–1369.
29. Motoshita J, Nakayama H, Taniyama K, Matsusaki K, Yasui W. Molecular characteristics of differentiated-type gastric carcinoma with distinct mucin phenotype: LI-cadherin is associated with intestinal phenotype. *Pathol Int* 2006; **56**: 200–205.
30. Tajima Y, Shimoda T, Nakanishi Y, Yokoyama N, Tanaka T, Shimizu K, *et al*. Association of gastric and intestinal phenotypic marker expression of gastric carcinomas with tumor thymidylate

synthase expression and response to postoperative chemotherapy with 5-fluorouracil. *J Cancer Res Clin Oncol* 2003; **129**: 683–690.
31. Ochiai A, Yasui W, Tahara E. Growth-promoting effect of gastrin on human gastric carcinoma cell line TMK-1. *Jpn J Cancer Res* 1985; **76**: 1064–1071.
32. Yanagihara K, Seyama T, Tsumuraya M, Kamada N, Yokoro K. Establishment and characterization of human signet ring cell gastric carcinoma cell lines with amplification of the c-myc oncogene. *Cancer Res* 1991; **51**: 381–386.
33. Sakamoto N, Oue N, Noguchi T, Sentani K, Anami K, Sanada Y, *et al*. Serial analysis of gene expression of esophageal squamous cell carcinoma: ADAMTS16 is up-regulated in esophageal squamous cell carcinoma. *Cancer Sci* (in press).

SUPPORTING INFORMATION ON THE INTERNET

The following supporting information may be found in the online version of this article.

Supplementary data. Materials and methods.

Relation between microRNA expression and progression and prognosis of gastric cancer: a microRNA expression analysis

Tetsuya Ueda, Stefano Volinia, Hiroshi Okumura, Masayoshi Shimizu, Cristian Taccioli, Simona Rossi, Hansjuerg Alder, Chang-gong Liu, Naohide Oue, Wataru Yasui, Kazuhiro Yoshida, Hiroki Sasaki, Sachiyo Nomura, Yasuyuki Seto, Michio Kaminishi, George A Calin, Carlo M Croce

Lancet Oncol 2010; 11: 136–46
Published Online December 21, 2009
DOI:10.1016/S1470-2045(09)70343-2
See Reflection and Reaction page 106

Department of Molecular Virology, Immunology, and Medical Genetics and Comprehensive Cancer Center, Ohio State University, Columbus, OH, USA (T Ueda MD, S Volinia PhD, H Okumura MD, C Taccioli PhD, H Alder PhD, Prof C-g Liu PhD, Prof C M Croce MD); **Department of Surgical Oncology and Digestive Surgery, Graduate School of Medicine and Dental Science, Kagoshima University, Kagoshima, Japan** (H Okumura); **Department of Gastrointestinal Surgery, Graduate School of Medicine, University of Tokyo, Tokyo, Japan** (T Ueda, S Nomura MD, Prof Y Seto MD, Prof M Kaminishi MD); **Department of Surgery, Showa General Hospital, Tokyo, Japan** (Prof M Kaminishi); **Department of Morphology and Embryology, University of Ferrara, Ferrara, Italy** (S Volinia, S Rossi PhD); **Department of Experimental Therapeutics, Division of Cancer Medicine, University of Texas MD Anderson Cancer Center, Houston, TX, USA** (M Shimizu BS, S Rossi, G A Calin MD, Prof C-G Liu); **Department of Molecular Pathology, Graduate School of Biomedical Sciences, Hiroshima University, Hiroshima, Japan** (N Oue MD, Prof W Yasui MD); **Department of Surgical Oncology, Research Institute for Radiation Biology and Medicine, Hiroshima University, Hiroshima, Japan** (Prof K Yoshida MD); **Department of Surgical Oncology, School of Medicine, Gifu University, Gifu, Japan** (Prof K Yoshida); **and Genetics Division, National Cancer Center Research Institute, Tokyo, Japan** (H Sasaki PhD)

Summary

Background Analyses of microRNA expression profiles have shown that many microRNAs are expressed aberrantly and correlate with tumorigenesis, progression, and prognosis of various haematological and solid tumours. We aimed to assess the relation between microRNA expression and progression and prognosis of gastric cancer.

Methods 353 gastric samples from two independent subsets of patients from Japan were analysed by microRNA microarray. MicroRNA expression patterns were compared between non-tumour mucosa and cancer samples, graded by diffuse and intestinal histological types and by progression-related factors (eg, depth of invasion, metastasis, and stage). Disease outcome was calculated by multivariable regression analysis to establish whether microRNAs are independent prognostic factors.

Findings In 160 paired samples of non-tumour mucosa and cancer, 22 microRNAs were upregulated and 13 were downregulated in gastric cancer; 292 (83%) samples were distinguished correctly by this signature. The two histological subtypes of gastric cancer showed different microRNA signatures: eight microRNAs were upregulated in diffuse-type and four in intestinal-type cancer. In the progression-related signature, miR-125b, miR-199a, and miR-100 were the most important microRNAs involved. Low expression of let-7g (hazard ratio 2·6 [95% CI 1·3–4·9]) and miR-433 (2·1 [1·1–3·9]) and high expression of miR-214 (2·4 [1·2–4·5]) were associated with unfavourable outcome in overall survival independent of clinical covariates, including depth of invasion, lymph-node metastasis, and stage.

Interpretation MicroRNAs are expressed differentially in gastric cancers, and histological subtypes are characterised by specific microRNA signatures. Unique microRNAs are associated with progression and prognosis of gastric cancer.

Funding National Cancer Institute.

Introduction

Gastric cancer is the fourth most common human malignant disease and the second most frequent cause of cancer-related death worldwide.[1] Improvement of diagnosis and treatment has resulted in good long-term survival for patients with early gastric cancer, whereas the outlook for individuals with advanced disease remains poor.[2] Advanced gastric cancer frequently recurs as nodal and haematogenous metastases and peritoneal dissemination. Although several types of non-surgical treatment have been assessed, surgical resection is still the primary curative treatment for localised gastric cancer.

Data from several studies show that various genetic alterations cause tumorigenesis and progression of gastric cancer.[3,4] Inactivation of runt-related transcription factor 3 (*RUNX3*) by methylation has also been reported.[5] Several groups have undertaken high-throughput analyses of gastric cancer expression profiles by DNA microarrays[4] and microdissection.[6] However, markers for tumorigenesis and progression of gastric cancer have not yet been discovered and specific therapeutic targets have not been identified.

A new class of small non-coding RNAs—microRNAs—has been discovered.[7] Mature microRNAs are composed of 19–25 nucleotides and are cleaved from 60–110-nucleotide hairpin microRNA precursors in the cytoplasm by the RNase III enzyme Dicer.[8] Single-stranded microRNAs bind mRNAs of potentially hundreds of genes at the 3′ untranslated region with imperfect complementarity, resulting in degradation of target mRNAs and inhibition of translation.[8] Several target-prediction programs have been developed, but very few targets have been proved experimentally.[9] MicroRNAs play a part in crucial cellular processes, including development, differentiation, stress response, apoptosis, and proliferation.[8,10] 475 human microRNAs have been reported to date (miRBase version 9.2; University of Manchester, Manchester, UK);[11] this number could reach 800–1000 through experimental confirmation of predicted microRNA genes.[12]

Microarray platforms have been developed for analysis of microRNA expression, and data show that several microRNAs are expressed aberrantly in various haematological and solid malignant diseases.[13–16] MicroRNAs act as novel oncogenes or tumour-suppressor genes.[17,18] We and others have noted that alterations in microRNA expression correlate highly with progression and prognosis of human tumours.[19–24] Thus, focusing on microRNAs in gastric cancer could yield new insights

into the biological behaviour of this disease. For oncogenic microRNAs, antagomirs are a type of antisense oligonucleotide that inhibit microRNA function in vivo effectively;[25–27] for tumour-suppressive microRNAs, reconstitution with microRNA precursor sequences has an antitumour effect. Therefore, microRNAs are possible therapeutic targets for cancer.[22,28]

To ascertain whether microRNA expression signatures can differ between gastric cancer and non-tumour mucosa, we undertook genome-wide microRNA expression profiling in two sets of gastric tissues. With expression-profile results for these samples and associated clinical variables, we investigated the association between microRNAs and histological types, tumour progression, and prognosis of gastric cancer.

Methods

Tissue samples

For microRNA expression profiling, we obtained gastric tissue samples (cancer lesions and adjacent non-tumour mucosae) from patients who underwent gastrectomy between 2002 and 2005 at the University of Tokyo (group 1) and between 1998 and 2005 at Hiroshima University (group 2). We gathered all samples in the same manner, and they were snap-frozen immediately in liquid nitrogen and stored at −80°C until RNA and protein extraction could be done. Since microdissection is difficult to do in diffuse-type gastric cancer, for technical uniformity we used bulk tissue for all cases.

We obtained study approval from the ethics committee at the University of Tokyo and every patient from the University of Tokyo gave written informed consent for samples to be used. Because we did not obtain written informed consent for samples from Hiroshima University, for strict privacy protection, identification information was removed before analysis; this procedure is in accordance with ethical guidelines for human genome or gene research enacted by the Japanese Government and was approved by the ethics review committee of the Hiroshima University School of Medicine.

Panel: Patient cohorts and of analyses undertaken

STEP 1: MicroRNA expression patterns in gastric cancer (non-tumour mucosa *vs* cancer)

Samples

61 pairs in group 1 and 99 in group 2 were analysed independently

Statistical methods

1 Class comparison by BRB-ArrayTools; paired *t* test ($p<0.01$)
2 Class prediction by BRB-ArrayTools; paired class prediction by the leave-one-out cross-validation method

Samples

169 non-tumour mucosae (64 samples from group 1 and 105 from group 2) and 184 cancers (81 samples from group 1 and 103 from group 2) (unpaired condition)

Statistical methods

Average linkage clustering with centred Pearson correlation with 35 microRNAs

STEP 2: MicroRNA expression patterns and histological types (diffuse-type *vs* intestinal-type gastric cancer)

Samples

103 diffuse-type and 81 intestinal-type gastric cancer samples

Statistical methods

1 Class comparison by BRB-ArrayTools; two-sample *t* test ($p<0.001$)
2 Average linkage clustering with centred Pearson correlation with the 19 most significant microRNAs ($p\leq 2\times10^{-6}$)

(Continues in next column)

(Continued from previous column)

STEP 3: MicroRNA expression and tumour progression correlation

Samples

- T3 and T4 *vs* T1 (101 *vs* 15 samples)
- Lymph-node metastasis (N) positive *vs* negative (126 *vs* 54 samples)
- Stage IV *vs* I (51 *vs* 37 samples)
- Peritoneal dissemination (P, CY) positive *vs* negative (33 *vs* 76 samples)
- Haematogenous metastasis (H, M) positive *vs* negative (12 *vs* 169 samples)

Statistical methods

1 Class comparison by BRB-ArrayTools; two-sample *t* test ($p<0.01$, for haematogenous metastasis, $p<0.05$)
2 Venn diagram of T, N, and stage
3 Significance analysis of microarrays (SAM) with rank-regression option for T and stage

STEP 4: MicroRNA expression and prognosis correlation

Samples

101 cases have information for disease outcome and underwent curative surgery. All 182 cases had surgery (curative or non-curative)

Overall survival

- Statistical methods
  1 Univariate Cox proportional hazards regression in BRB-ArrayTools
  2 Kaplan-Meier survival curves
  3 Multivariable Cox proportional hazards regression analysis

Disease-free survival

- Statistical methods
  1 Univariate Cox proportional hazards regression in BRB-ArrayTools
  2 Kaplan-Meier survival curves
  3 Multivariable Cox proportional hazards regression analysis

Correspondence to:
Prof Carlo M Croce, Department of Molecular Virology, Immunology, and Medical Genetics and Comprehensive Cancer Center, Ohio State University, Biomedical Research Tower, Room 1080, 460 W 12th Ave, Columbus, OH 43210, USA
carlo.croce@osumc.edu

For **miRBase** see http://www.mirbase.org